# A fourth-order numerical method for the planetary geostrophic equations with inviscid geostrophic balance

**Roger Samelson · Roger Temam · Cheng Wang ·
Shouhong Wang**

**Abstract** The planetary geostrophic equations with inviscid balance equation are reformulated in an alternate form, and a fourth-order finite difference numerical method of solution is proposed and analyzed in this article. In the reformulation, there is only one prognostic equation for the temperature field and the velocity field is statically determined by the planetary geostrophic balance combined with the incompressibility condition. The key observation is that all the velocity profiles can be explicitly determined by the temperature gradient, by utilizing the special form of the Coriolis parameter. This brings convenience and efficiency in the numerical study. In the fourth-order scheme, the temperature is dynamically updated at the regular numerical grid by long-stencil approximation, along with a one-sided extrapolation near the boundary. The velocity variables are recovered by special solvers on the 3-D staggered

R. Samelson
College of Oceanic and Atmospheric Sciences, Oregon State University,
Corvallis, OR 97331-5503, USA
e-mail: rsamelson@coas.oregonstate.edu

R. Temam · S. Wang
Institute for Scientific Computing and Applied Mathematics & Department of Mathematics,
Indiana University, Bloomington, IN 47405-5701, USA
e-mail: temam@indiana.edu

S. Wang
e-mail: showang@indiana.edu

C. Wang (✉)
Department of Mathematics, University of Tennessee, Knoxville, TN 37996-1300, USA
e-mail: wang@math.utk.edu

grid. Furthermore, it is shown that the numerical velocity field is divergence-free at the discrete level in a suitable sense. Fourth order convergence is proven under mild regularity requirements.

**Mathematics Subject Classification (2000)**   35Q35 · 65M06 · 65M12 · 86A10

## 1 Introduction

The primary purpose of this article is to propose a fourth-order numerical method for the planetary geostrophic equations (PGEs) with an inviscid balance equation. In addition, the fourth-order convergence analysis is provided under an appropriate regularity assumption for the exact solution.

The PGEs have been used in large-scale ocean circulation since the pioneering work of Welander [29] and Robinson and Stommel [16]. This system arises as an asymptotic approximation to the primitive equations (PEs) for planetary-scale motions in the limit of small Rossby number. One of the most distinguishing features is that there is only one prognostic equation in the system for the temperature field; the velocity field is diagnostically determined by the planetary geostrophic balance.

We consider the original formulation of the PGEs, with no viscous term in the geostrophic balance equations. The viscous case has been discussed in earlier literatures [2,19,20]. However, the inviscid geostrophic balance presents a serious challenge, since regularity estimates are not available for the vertical velocity by a direct manipulation. To overcome this difficulty, we consider an equivalent formulation of the original PGE system. The key point is that both horizontal and vertical velocity profiles are represented in terms of the temperature gradient, by utilizing the planetary geostrophic balance. The horizontal velocity turns out to be the solution of a differential equation at each fixed horizontal point, depending only on the temperature gradient. The vertical velocity is recovered by the continuity equation. In more detail, a two-point boundary value ordinary differential equations (ODE) in the vertical direction can be derived for the vertical velocity at each fixed horizontal point, with the right-hand side depending only on the first-order derivative of the temperature field. This is crucial to the well-posedness of the reformulated system. See a recent article by Liu et al. [10].

Thanks to the new formulation, stable, efficient and accurate numerical methods can be derived. We consider a fourth-order scheme in this article, since this is a widely accepted way to improve the accuracy within limited resolution, due to the enormous scale of the three-dimensional setting. Regarding the spatial discretization, at each time step (stage), the temperature field is dynamically updated at the regular numerical grid using fourth-order long stencil differences, with a one-sided extrapolation to obtain the "ghost" point values near each boundary section. The velocity variables, which are located at a 3-D staggered grid known as the marker and cell (MAC) grid, are statically determined by a special procedure. The horizontal velocity field is recovered by vertical integration of the temperature orthogonal gradient at the discrete level (with the Coriolis parameter on the denominator because of the geostrophic balance), combined with the constraint regarding its discrete average in the vertical direction. The vertical velocity is solved by a discrete realization of the two-point

boundary value ODE, in which the source term is merely related to the horizontal derivative of the temperature field and the Coriolis force parameter evaluated at the corresponding staggered grid. To reduce the computational effort, we use compact difference operators to approximate the derivatives in the vertical direction. The source term appearing in the compact difference equations to determine the vertical velocity, which is a fourth-order approximation to the original ODE, is chosen to ensure that the numerical velocity field satisfies the divergence-free property in a weaker sense. This is remarkable since for the usual discretizations of the Navier–Stokes or Maxwell equations, only second-order difference methods, such as the usual MAC scheme or Yee scheme, can achieve the divergence-free condition for the velocity field at the discrete level. A relevant discussion can be found e.g., in [12].

It is the first time that one derives a fourth-order method on a staggered grid, especially for a 3-D oceanic flow calculation. In the classical MAC schemes, the difficulty of solving for the pressure, the staggered location of different physical variables, and the treatment of the boundary conditions make a fourth-order finite difference scheme infeasible. In this article, the pressure variable is eliminated in the reformulation, and each velocity variable is determined by the temperature gradient. Moreover, the suitable usage of both the long-stencil and compact operators, along with the high-order one-sided extrapolation around the boundary, avoids the difficulty related to the boundary conditions. In addition, the theoretical fourth-order convergence of the spatial discretization scheme is established in the article.

The temporal discretization is also discussed. The nonlinear convection term is updated explicitly and the thermal diffusion terms can be treated by either an implicit approach, such as the Crank–Nicholson method, or by an explicit multi-stage time approach, such as the classical fourth-order Runge-Kutta method. Both approaches lead to a stable and accurate method as shown in the accuracy check using smooth test solutions. The main computations reduce to the evolution of a convection-diffusion equation and the recovery procedures for the horizontal and vertical velocities, thus providing an efficient numerical scheme.

In addition, the convergence analysis of the proposed numerical method is provided in this article. Due to the special feature of the alternate formulation, the nonlinearity of the temperature transport equation is overcome by the fact that the velocity is controlled by the temperature gradient. As a result, the methodology to analyze a regular convection–diffusion equation can be applied in a convenient way. The analysis of the temporal discretization to deal with convection–diffusion equation, either a Crank–Nicholson or forward Euler, is standard. We omit the detail in this article for brevity of presentation. In other words, we only look at the spatial discretization, i.e., method of lines, in the fourth-order convergence analysis. The consistency analysis is carried out by constructing approximate solutions to satisfy the numerical scheme up to an $O(h^4)$ accuracy and the corresponding error estimate. A cancellation methodology in the approximation is explored, to avoid a typical difficulty arising in the analysis of finite difference methods, if a direct truncation error estimate is performed. Subsequently, the error analysis is implemented by the energy estimate of the temperature error equation. The stability of the numerical scheme is indicated by the fact that the numerical difference operators appearing in the long-stencil operator are well-posed.

This article is organized as follows. The derivation of the alternate formulation for the PGEs is recalled in Sect. 2. The fourth-order numerical method, including spatial discretization of the transport equation on a regular grid, the determination of the velocity field on the staggered grid, and the time stepping, is presented in Sect. 3. Section 4 gives a numerical accuracy check for the numerical scheme. The convergence analysis for the fourth-order scheme is provided in Sect. 5.

## 2 Review of an alternate formulation of the inviscid PGEs

The PGEs can be written in a non-dimensional form

$$
\begin{cases}
\partial_t T + (\boldsymbol{v}\cdot\nabla)T + w\frac{\partial T}{\partial z} = \left(\frac{1}{Rt_1}\triangle + \frac{1}{Rt_2}\partial_z^2\right)T, \\
f k \times \boldsymbol{v} + \nabla p = F, \\
\frac{\partial p}{\partial z} = T, \\
\nabla\cdot\boldsymbol{v} + \partial_z w = 0,
\end{cases}
\tag{2.1}
$$

where $T$ represents the temperature, $\boldsymbol{u} = (\boldsymbol{v}, w) = (u, v, w)$ the velocity, and $p$ the pressure. The term $f k \times \boldsymbol{v} = f\binom{-v}{u}$ corresponds to the Coriolis force with $f$ depending only on the latitude $y$. As a typical example used in the geophysical literature, its $\beta$−plane approximation is given by $f = f_0 + \beta y$, where $f_0$ and $\beta$ are constants. For simplicity, we set $\kappa_1 = 1/Rt_1$, $\kappa_2 = 1/Rt_2$, which stand for the horizontal and vertical thermal diffusivity. To avoid confusion, we use the operators $\nabla$, $\nabla^\perp$, $\nabla\cdot$, $\triangle$ to denote the gradient, perpendicular gradient, divergence and Laplacian in the horizontal plane, respectively. The forcing term $F = (F^x, F^y)^\perp$ appearing in the geostrophic balance equation $(2.1)_2$ comes from the wind stress at the ocean surface, which is a boundary layer approximation. It may or may not depend on the vertical variable $z$. For simplicity, we assume in this article that $F = F(x, y) = (F^x(x, y), F^y(x, y))$. The discussion of a general case can be carried out in the same fashion. See the relevant references on both the physical and mathematical descriptions of the PGEs in [3–5, 13–17, 19–24, 29], etc.

The computational domain is taken as $\mathcal{M} = \mathcal{M}_0 \times [-H_0, 0]$, $\mathcal{M}_0$ being the surface of the ocean. The boundary condition at the top and bottom surfaces are given by

$$
\begin{aligned}
w = 0 \quad \text{and} \quad \kappa_2 \frac{\partial T}{\partial z} = T^f, \quad \text{at } z = 0, \\
w = 0 \quad \text{and} \quad \kappa_2 \frac{\partial T}{\partial z} = 0, \quad \text{at } z = -H_0.
\end{aligned}
\tag{2.2}
$$

Usually the heat flux term $T^f$ at the ocean surface can be taken as either a fixed heat flux function or of the form $T^f = -\alpha(T - \theta^*)$, with $\theta^*$ being a reference temperature. For simplicity we choose $T^f$ as a given flux. On the lateral boundary, the temperature field is prescribed

$$
T = T_{lb}, \quad \text{on } \partial\mathcal{M}_0 \times [-H_0, 0],
\tag{2.3}
$$

where $T_{lb}$ is given. The purpose of this choice is a simplification of the analysis of the system, although the no-flux boundary condition for the temperature field is physically more relevant. It can also be viewed as an approximation such that the disturbance of oceanic circulation motion is far away from the lateral boundary. For the sake of simplicity in the presentation, we set the homogeneous profile $T_{lb} = 0$ in the numerical analysis. There is no real change for the non-homogeneous case. The normal component of the vertically averaged horizontal velocity turns out to have a vanishing flux

$$\bar{\boldsymbol{v}} \cdot \boldsymbol{n} = 0, \quad \text{on } \partial \mathcal{M}_0, \tag{2.4}$$

which is compatible with the continuity equation $(2.1)_4$. We recall that the average (in the vertical direction) of any 3-D field $g$ is given by $\bar{g}(x, y) = \frac{1}{H_0} \int_{-H_0}^{0} g(x, y, z) dz$. See Pedlosky [14] and Samelson et al. [19] for a detailed explanation for the choice of this nonlocal boundary condition in the case where no viscosity is present in the geostrophic balance equation.

The PGEs with viscous geostrophic balance have been analyzed in recent articles; see Cao and Titi [2], Samelson et al. [19,20], etc. The difficulty of the original system (2.1) (with no diffusion term in the geostrophic balance equation) is due to the lack of regularity for the velocity field, as discussed in detail in [20]. In this article, we consider an equivalent formulation of Eqs. (2.1)–(2.4) to facilitate the numerical study. The key point in this reformulation is that both the horizontal and vertical velocity variables can be determined by the first-order derivative of the temperature field.

Indeed, the horizontal velocity field is the solution of the following system

$$\begin{cases} \partial_z u = \frac{-T_y}{f}, \quad \partial_z v = \frac{T_x}{f}, \\ \bar{u}(x, y) = \bar{u}_e, \quad \bar{v}(x, y) = \bar{v}_e = \frac{-\partial_y F^x + \partial_x F^y}{\partial_y f}, \end{cases} \tag{2.5}$$

where $\bar{u}_e$ is explicitly given by Eq. (2.8) below.

Equation $(2.5)_1$, the thermal wind equation, is derived by taking the vertical derivative of the geostrophic balance equation $f k \times \boldsymbol{v} + \nabla p = F$. Note that the hydrostatic balance $\partial p / \partial z = T$ and the independence on $z$ of $F$ and $f = f(y)$ were used. Meanwhile, averaging the geostrophic balance equation $f k \times \boldsymbol{v} + \nabla p = F$ in the vertical direction leads to

$$f k \times \bar{\boldsymbol{v}} + \nabla \bar{p} = F. \tag{2.6}$$

Applying the curl operator $\nabla^\perp$ to Eq. (2.6) results in

$$(\partial_y f)\bar{v} + f(\bar{v}_y + \bar{u}_x) = (\partial_y f)\bar{v} = \nabla \times F = -\partial_y F^x + \partial_x F^y, \tag{2.7a}$$

which in turn yields

$$\bar{v}_e = \bar{v}(x, y) = \frac{-\partial_y F^x + \partial_x F^y}{\partial_y f}. \tag{2.7b}$$

The second step of Eq. (2.7a) utilizes the fact that the averaged horizontal velocity field is divergence-free, that is $\nabla \cdot \overline{\boldsymbol{v}} = 0$, which comes from the continuity equation $\nabla \cdot \boldsymbol{v} + \partial_z w = 0$ and the boundary condition for the vertical velocity $w(\cdot, 0) = w(\cdot, -H_0) = 0$.

The vertically averaged horizontal velocity $\overline{u}_e$ is determined by $\overline{v}_e$ given by Eq. (2.7b). Because of the divergence-free property of the profile $\overline{\boldsymbol{v}}$, we can find a 2-D mean stream function $\overline{\psi}(x, y)$, such that $(\overline{u}, \overline{v}) = (-\partial_y \overline{\psi}, \partial_x \overline{\psi})$. Moreover, the boundary condition (2.4) indicates that $\overline{\psi}$ is constant on the lateral boundary. We can set $\overline{\psi} = 0$ on $\partial \mathcal{M}_0$. In addition, we denote by $\gamma_1(y_0)$, $\gamma_2(y_0)$ the $x$-coordinates of the intersection points between $\partial \mathcal{M}_0$ and $y = y_0$. The mean stream function $\overline{\psi}$ and the mean velocity $\overline{u}$ can be determined by the kinematic relationship and formula (2.7b):

$$\overline{\psi}_e(x, y) = \int_{\gamma_1(y)}^{x} \frac{\nabla \times F}{\partial_y f} \, dx', \quad \overline{u}_e(x, y) = -\partial_y \overline{\psi}_e(x, y), \tag{2.8}$$

where $\gamma_1(y)$ is a point on $\partial \mathcal{M}_0$. Evaluating $\overline{\psi}$ at another boundary point $(\gamma_2(y), y)$ with the same $y$-value, we obtain an additional constraint on the forcing:

$$\int_{\gamma_1(y)}^{\gamma_2(y)} \frac{\nabla \times F}{\partial_y f} \, dx' = 0, \tag{2.9}$$

since $\overline{\psi}$ is identically 0 on the lateral boundary. Constraint (2.9) amounts to saying that the average forcing across the domain at a fixed $y$ must not give a torque on the fluid.

The vertical velocity can also be represented as the solution of a differential equation. By taking the vertical derivative of the continuity equation

$$\nabla \cdot \boldsymbol{v}_z + \partial_z^2 w = 0, \tag{2.10}$$

and recalling the thermal wind equation (2.5)$_1$, we arrive at

$$\partial_z^2 w = -\partial_x(u_z) - \partial_y(v_z) = \partial_x \left( \frac{T_y}{f} \right) - \partial_y \left( \frac{T_x}{f} \right) = \frac{(\partial_y f) T_x}{f^2}. \tag{2.11}$$

Note that the second-order derivatives for the temperature field cancel each other due to the special form of the Coriolis parameter $f = f(y)$. Then we have the following system of second-order ODEs

$$\begin{cases} \partial_z^2 w = \frac{(\partial_y f) T_x}{f^2}, \\ w = 0, \quad \text{at } z = 0, -H_0, \end{cases} \tag{2.12}$$

in which the right hand side includes only the first-order derivative of the temperature.

The PGEs with inviscid balance equation can now be formulated as follows.

*Temperature transport equation*

$$
\begin{cases}
T_t + (\boldsymbol{v}\cdot\nabla)T + w\frac{\partial T}{\partial z} = \left(\kappa_1\triangle + \kappa_2\partial_z^2\right)T, \\
\frac{\partial T}{\partial z} = \frac{T_f}{\kappa_2}, \quad \text{at } z = 0, \quad \frac{\partial T}{\partial z} = 0, \quad \text{at } z = -H_0, \\
T = 0, \quad \text{on } \partial\mathcal{M}_0 \times [-H_0, 0];
\end{cases}
\tag{2.13a}
$$

*Recovery of the horizontal velocity*

$$
\begin{cases}
\partial_z u = -\frac{T_y}{f}, \quad \partial_z v = \frac{T_x}{f}, \\
\bar{u}(x, y) = \bar{u}_e, \quad \bar{v}(x, y) = \bar{v}_e;
\end{cases}
\tag{2.13b}
$$

*Recovery of the vertical velocity*

$$
\begin{cases}
\partial_z^2 w = \frac{(\partial_y f)T_x}{f^2}, \\
w = 0, \quad \text{at } z = 0, -H_0.
\end{cases}
\tag{2.13c}
$$

The well-posedness of this reformulation at the PDE level was analyzed in a recent article by Liu et al. [10], in which the global existence of weak solution was proven.

## 3 The fourth-order numerical scheme

The methodology of the numerical scheme follows the derivation of the alternate formulation (2.13). At each time step (stage), the temperature field is first updated at regular numerical grid, using centered difference approximations. Subsequently, the horizontal and vertical velocities are determined by discrete realizations of the differential equations (2.13b) and (2.13c), respectively.

For simplicity of the presentation, we consider the homogeneous forcing term $F = 0$ in the geostrophic balance and wind stress $T_f = 0$ in the temperature boundary condition hereafter. The case with non-homogeneous force term or wind stress can be dealt with in the same fashion and does not add any mathematical difficulty.

A fourth-order numerical scheme has an obvious advantage over the standard second-order centered difference scheme, because of the enormous scale of the three-dimensional setting. However, the difficulty of numerical stability (especially near the boundary) may lead to a numerical artifact, as shown in many earlier articles. Furthermore, the efficiency of the numerical implementation of a fourth-order method has always been another challenging issue. See the detailed discussions in e.g., Anderson and Reider [1], Henshaw et al. [8], E and Liu [6].

A new methodology is utilized in this article to deal with a fourth-order scheme for the 3-D PGEs formulated in (2.13). The temperature variable is located at the regular grid and the velocity variables are evaluated at the 3-D staggered grid. The spatial derivatives of the temperature transport equation is approximated with fourth-order
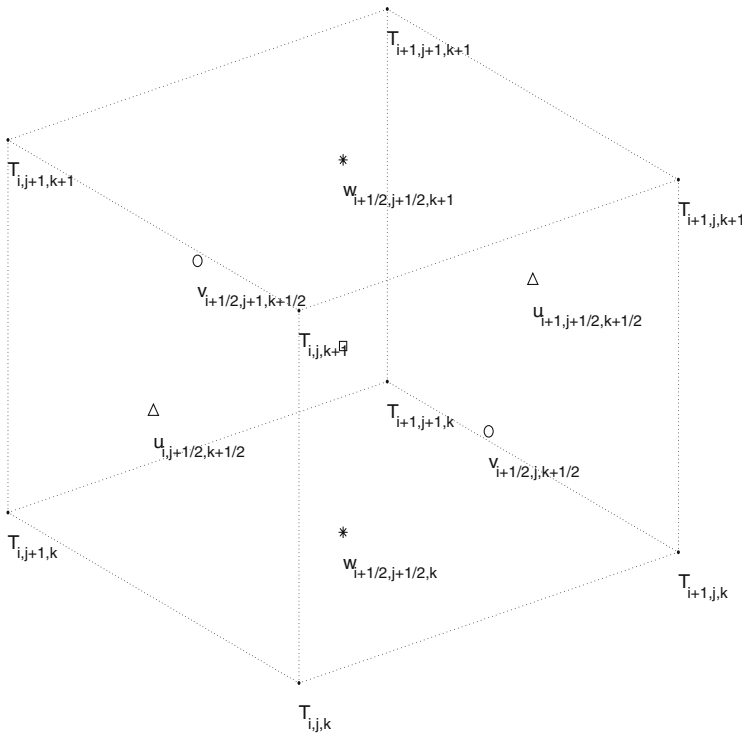
**Fig. 1** The 3-D MAC grid for the PGEs

accuracy by long stencil differences, with the "ghost" point values recovered by one-sided extrapolation near the boundary. Such an extrapolation is accomplished by using information from the original PDE, to reduce the number of interior points needed in the one-sided formula for better stability property. Subsequently, both the horizontal and vertical velocity variables are determined on the staggered grid by the data of temperature gradient, which are calculated by long stencil differences, via compact difference equations.

The main computation efforts in the fourth-order scheme at each time step (stage) reduce to this: explicit long stencil finite difference updating in the temperature transport equation, along with fourth-order recovery for the velocity field. This makes the scheme efficient and accurate.

It is assumed that $\mathcal{M}_0 = [0, 1]^2$ and $\triangle x = \triangle y = \triangle z = h$. The temperature variable is evaluated at the regular numerical grid points $(x_i, y_j, z_k)$; see Fig. 1. In order to assure the divergence-free property of the computed velocity field at the discrete level in an appropriate sense, we choose a staggered grid for the velocity field, in which $\boldsymbol{u} = (\boldsymbol{v}, w) = (u, v, w)$ are evaluated at the mesh points $(i, j \pm 1/2, k \pm 1/2)$, $(i \pm 1/2, j, k \pm 1/2)$, $(i \pm 1/2, j \pm 1/2, k)$, respectively. More precisely, the $u$ velocity is located at the triangle points, the $v$ velocity at the circle points, and the $w$ velocity at the star points. This staggered grid is also known as the 3-D MAC grid, whose 2-D version was first proposed by Harlow and Welch in [7] to deal with the numerical

solution of the NSEs. Its advantage here will be addressed in Sect. 3.4. A similar staggered grid was proposed and analyzed in a recent article by Samelson et al. [18] to deal with the 3-D PEs. Its relationship with a regular numerical grid based on the vorticity formulation was discussed in [25–27].

Before the formal discussion of the scheme, we introduce some finite difference and average operators to simplify the explanations below. The following notations of centered differences using different stencils at different grid points are introduced to facilitate the description:

$$
\begin{aligned}
D_x g(x) &= \frac{g\left(x + \frac{1}{2}\Delta x\right) - g\left(x - \frac{1}{2}\Delta x\right)}{\Delta x}, \\
\tilde{D}_x g(x) &= \frac{g(x + \Delta x) - g(x - \Delta x)}{2\Delta x}, \\
D_x^2 g(x) &= \frac{g(x - \Delta x) - 2g(x) + g(x + \Delta x)}{\Delta x^2},
\end{aligned}
\tag{3.1}
$$

$$
\begin{aligned}
&D_x \left(1 - \frac{\Delta x^2}{24} D_x^2\right) g(x) \\
&= \frac{g\left(x - \frac{3}{2}h\right) - 27g\left(x - \frac{1}{2}h\right) + 27g\left(x + \frac{1}{2}h\right) - g\left(x + \frac{3}{2}h\right)}{24\Delta x},
\end{aligned}
\tag{3.2a}
$$

$$
\begin{aligned}
&\tilde{D}_x \left(1 - \frac{\Delta x^2}{6} D_x^2\right) g(x) \\
&= \frac{g(x - 2h) - 8g(x - h) + 8g(x + h) - g(x + 2h)}{12\Delta x},
\end{aligned}
\tag{3.2b}
$$

$$
\begin{aligned}
&D_x^2 \left(1 - \frac{\Delta x^2}{12} D_x^2\right) g(x) \\
&= \frac{-g(x - 2h) + 16g(x - h) - 30g(x) + 16g(x + h) - g(x + 2h)}{12\Delta x^2}.
\end{aligned}
\tag{3.3}
$$

It can be easily verified by a careful Taylor expansion that both long-stencil operators in (3.2) are fourth-order approximations to $\partial_x$, and the operator in Eq. (3.3) is a fourth-order approximation to $\partial_x^2$. Note that Eqs. (3.2b) and (3.3) are the standard long stencil differences on a regular grid, while Eq. (3.2b) is evaluated for variables located at a staggered grid. The corresponding operator in the $y$ and $z$ directions can be defined in a similar way. We omit the details here.

Moreover, because of the staggered grid used in the scheme, the following fourth-order average operator is needed to interpolate the numerical values of the different

physical variables at a special mesh point:

$$\mathcal{A}_x g(x) = -\frac{1}{16} g\left(x - \frac{3}{2}h\right) + \frac{9}{16} g\left(x - \frac{1}{2}h\right) + \frac{9}{16} g\left(x + \frac{1}{2}h\right) - \frac{1}{16} g\left(x + \frac{3}{2}h\right).$$

(3.4)

The analogous definitions of $\mathcal{A}_y$, $\mathcal{A}_z$ can be similarly given.

### 3.1 Update of the temperature in the PGEs: method of lines

Regarding the temperature variable, the fourth-order long-stencil differences (3.2b), (3.3) are used to replace the derivatives in the transport equation (2.13a) at each grid point $(i, j, k)$, $1 \leq i, j \leq N - 1$, $0 \leq k \leq N_z$. In other words, the method of lines gives

$$\partial_t T + \mathcal{N}_h(\mathbf{u}, T) = \left(\kappa_1 \left(D_x^2 - \frac{h^2}{12} D_x^4 + D_y^2 - \frac{h^2}{12} D_y^4\right) + \kappa_2 \left(D_z^2 - \frac{h^2}{12} D_z^4\right)\right) T, \quad \text{at } (i, j, k),$$

(3.5)

with the nonlinear convection term

$$\mathcal{N}_h(\mathbf{u}, T) = \bar{\bar{u}} \tilde{D}_x \left(1 - \frac{h^2}{6} D_x^2\right) T + \bar{\bar{v}} \tilde{D}_y \left(1 - \frac{h^2}{6} D_y^2\right) T + \bar{\bar{w}} \tilde{D}_z \left(1 - \frac{h^2}{6} D_z^2\right) T,$$

(3.6)

and average values of $u$, $v$, $w$ at the regular mesh points given by:

$$\bar{\bar{u}}_{i,j,k} = \mathcal{A}_y(\mathcal{A}_z u)_{i,j,k}, \quad \bar{\bar{v}}_{i,j,k} = \mathcal{A}_x(\mathcal{A}_z v)_{i,j,k}, \quad \bar{\bar{w}}_{i,j,k} = \mathcal{A}_x(\mathcal{A}_y w)_{i,j,k}. \quad (3.7)$$

### 3.1.1 Ghost point values for T

Due to the Neumann boundary condition imposed on the top and bottom, the temperature on the boundary is not known explicitly, only its normal derivative. Consequently, the determination of "ghost" point values, e.g., $T_{i,j,-1}$ and $T_{i,j,-2}$ around the bottom boundary section $z = -H_0$, is required.

We begin by deriving one-sided approximations. A local Taylor expansion near the bottom boundary $z = -H_0$ gives

$$T_{i,j,-1} = T_{i,j,1} - 2\Delta z \partial_z T_{i,j,0} - \frac{\Delta z^3}{3} \partial_z^3 T_{i,j,0} + O(h^5),$$

$$T_{i,j,-2} = T_{i,j,2} - 4\Delta z \partial_z T_{i,j,0} - \frac{8\Delta z^3}{3} \partial_z^3 T_{i,j,0} + O(h^5),$$

(3.8)

in which the term $\partial_z T_{i,j,0}$ is known to vanish because of the no-flux boundary condition for the temperature. The remaining work is focused on the determination of $\partial_z^3 T$ at

$k = 0$, for which we use information from the original PDE and its derivatives. More precisely, applying the vertical derivative $\partial_z$ to the temperature transport equation leads to

$$T_{zt} + u_z T_x + u T_{zx} + v_z T_y + v T_{zy} + w_z T_z + w T_{zz}$$
$$= \kappa_1 (T_{zxx} + T_{zyy}) + \kappa_2 \partial_z^3 T, \quad \text{at } z = -H_0. \tag{3.9}$$

Using the no-flux boundary condition for $T$ and the vanishing boundary condition for $w$ at $z = -H_0$, we have

$$\partial_z^3 T = \frac{1}{\kappa_2} \left( u_z T_x + v_z T_y \right), \quad \text{at } z = -H_0, \tag{3.10}$$

which combined with the geostrophic balance $(u_z, v_z) = (-\partial_y T/f, \partial_x T/f)$ results in

$$\partial_z^3 T = 0, \quad \text{at } z = -H_0. \tag{3.11}$$

Inserting Eq. (3.11) into Eq. (3.8) shows that

$$T_{i,j,-1} = T_{i,j,1} + O(h^5), \quad T_{i,j,-2} = T_{i,j,2} + O(h^5). \tag{3.12}$$

Analogous formulas for one-sided extrapolations of $T_{i,j,N_z+1}, T_{i,j,N_z+2}$ around the top boundary $z = 0$ can be derived in a similar way. The evaluation of the vertical derivative of the transport equation as shown in Eq. (3.9) is still valid. Furthermore, the heat flux boundary condition at the top $z = 0$, combined with the average approximation (3.4) gives

$$\partial_z^3 T = \frac{1}{\kappa_2^2} \left( \mathcal{A}_y (\mathcal{A}_z u) \partial_x (T^f) + \mathcal{A}_x (\mathcal{A}_z v) \partial_y (T^f) \right.$$
$$\left. + \mathcal{A}_x (\mathcal{A}_y \tilde{D}_z w) T^f \right) + O(h^2), \quad \text{at } z = 0, \tag{3.13}$$

with the average operators $\mathcal{A}_x, \mathcal{A}_y, \mathcal{A}_z$ given by Eq. (3.4). Therefore, we arrive at the extrapolation formulas around the top boundary

$$T_{i,j,N_z+1} = T_{i,j,N_z-1} + 2\Delta z (T^f)_{i,j,N} + \frac{\Delta z^3}{3\kappa_2^2} \left( \mathcal{A}_y (\mathcal{A}_z u) \partial_x (T^f) + \mathcal{A}_x (\mathcal{A}_z v) \partial_y (T^f) \right.$$
$$\left. + \mathcal{A}_x (\mathcal{A}_y \tilde{D}_z w) T^f \right)_{i,j,N} + O(h^5),$$

$$T_{i,j,N_z+2} = T_{i,j,N_z-2} + 4\Delta z (T^f)_{i,j,N} + \frac{8\Delta z^3}{3\kappa_2^2} \left( \mathcal{A}_y (\mathcal{A}_z u) \partial_x (T^f) + \mathcal{A}_x (\mathcal{A}_z v) \partial_y (T^f) \right.$$
$$\left. + \mathcal{A}_x (\mathcal{A}_y \tilde{D}_z w) T^f \right)_{i,j,N} + O(h^5). \tag{3.14}$$

On the lateral boundary sections, the homogeneous Dirichlet boundary condition for the temperature implies its numerical realization

$$T_{0,j,k} = 0, \quad T_{N,j,k} = 0, \quad T_{i,0,k} = 0, \quad T_{i,N,k} = 0. \tag{3.15}$$

In addition, the determination of $T$ at one "ghost" point, e.g., $T_{-1,j,k}$ around the left boundary section $x = 0$ (corresponding to the grid $i = 0$), is needed to implement the fourth-order difference scheme (3.5). We utilize a similar idea as that of Wang et al. [11,28], in which a fourth-order scheme for the 2-D Boussinesq system in vorticity formulation was studied. A local Taylor expansion of the fifth-order near the boundary gives

$$T_{-1,j,k} = \frac{20}{11}T_{0,j,k} - \frac{6}{11}T_{1,j,k} - \frac{4}{11}T_{2,j,k} + \frac{1}{11}T_{3,j,k} + \frac{12}{11}\triangle x^2 \partial_x^2 T_{i,j,0} + O(h^5). \tag{3.16}$$

The realization of Eq. (3.16) requires an accurate evaluation of $\partial_x^2 T$ at $i = 0$. Such a term can be determined by considering the original temperature transport equation evaluated on the boundary

$$\partial_t T \mid_{i=0} + (u\partial_x T) \mid_{i=0} + (v\partial_y T) \mid_{i=0} + (w\partial_z T) \mid_{i=0}$$
$$= \kappa_1 (\partial_x^2 T) \mid_{i=0} + (\kappa_1 \partial_y^2 + \kappa_2 \partial_z^2) T \mid_{i=0}. \tag{3.17}$$

Note that the following terms vanish on the left boundary

$$\partial_t T = 0, \quad \partial_y^2 T = 0, \quad \partial_z^2 T = 0, \quad v\partial_y T = 0, \quad w\partial_z T = 0, \quad \text{at } x = 0, \tag{3.18}$$

which comes from the homogeneous Dirichlet boundary condition for $T$. Moreover, the normal velocity component of $u$ also vanishes on the boundary, due to the determination of the horizontal velocity given by Eq. (2.13b)

$$\partial_z u = -\frac{\partial_y T}{f(y)} = 0, \quad \bar{u} = 0, \quad \text{at } x = 0. \tag{3.19}$$

As a result, we have

$$u \mid_{x=0} = 0, \quad \text{which implies} \quad (u\partial_x T) \mid_{x=0} = 0. \tag{3.20}$$

The combination of Eqs. (3.18), (3.20) and (3.17) shows that

$$\partial_x^2 T = 0, \quad \text{at } x = 0. \tag{3.21}$$

Going back to Eq. (3.16), we arrive at the following fifth-order approximation for the temperature at the "ghost" point:

$$T_{-1,j,k} = \frac{20}{11}T_{0,j,k} - \frac{6}{11}T_{1,j,k} - \frac{4}{11}T_{2,j,k} + \frac{1}{11}T_{3,j,k} + O(h^5). \tag{3.22}$$

The one sided extrapolation for $T$ around the three other lateral boundary sections can be derived in a similar way. The details are omitted.

$$T_{N+1,j,k} = \frac{20}{11}T_{N,j,k} - \frac{6}{11}T_{N-1,j,k} - \frac{4}{11}T_{N-2,j,k} + \frac{1}{11}T_{N-3,j,k} + O(h^5),$$

$$T_{i,-1,k} = \frac{20}{11}T_{i,0,k} - \frac{6}{11}T_{i,1,k} - \frac{4}{11}T_{i,2,k} + \frac{1}{11}T_{i,3,k} + O(h^5), \qquad (3.23)$$

$$T_{i,N+1,k} = \frac{20}{11}T_{i,N,k} - \frac{6}{11}T_{i,N-1,k} - \frac{4}{11}T_{i,N-2,k} + \frac{1}{11}T_{i,N-3,k} + O(h^5).$$

### 3.2 Recovery of the horizontal velocity field

After the numerical values for the temperature $T$ at the regular mesh grid points are determined by the finite difference method outlined above, the vertical derivative of the horizontal velocity $v_z$ is given by $(-\partial_y T/f, \partial_x T/f)$ as indicated by Eq. (2.13b). For simplicity, we use the $\beta$-plane approximation $f = f_0 + \beta y$.

As shown in Fig. 1, the discrete derivatives of the horizontal velocity $v = (u, v)$ in the vertical direction are evaluated at the mesh point $(i, j + 1/2, k + 1/2)$, $(i + 1/2, j, k+1/2)$, respectively. Yet, a straightforward fourth-order approximation of $\partial_z$ using the long stencil operator as in Eq. (3.2b) would lead to a linear system difficult to solve. To reduce the computational effort, we aim to introduce a compact fourth-order solver so that a recovery procedure can be efficiently applied. A fourth-order Taylor expansion in the vertical direction shows that

$$D_z = \partial_z + \frac{\Delta z^2}{24}\partial_z^3 + O(h^4) = \partial_z\left(1 + \frac{\Delta z^2}{24}\partial_z^2\right) + O(h^4) = \partial_z\left(1 + \frac{\Delta z^2}{24}D_z^2\right) + O(h^4),$$

$$(3.24)$$

which in turn gives a compact approximation to $\partial_z$

$$\partial_z = \frac{D_z}{1 + \frac{\Delta z^2}{24}D_z^2} + O(h^4). \qquad (3.25)$$

Note that at $z = z_k$, $D_z$ requires the grid $z_{k-1/2}$, $z_{k+1/2}$, and $D_z^2$ requires the values at $z_{k-1}$, $z_k$, $z_{k+1}$. That is the reason it is called a compact operator. On the other hand, the fourth-order long stencil difference (3.2b) can be chosen to approximate the source term of Eq. (2.13b)

$$-\left(\frac{\partial_y T}{f}\right)_{i,j+1/2,k} = -\frac{1}{f_0 + \beta y_{j+1/2}}D_y\left(1 - \frac{h^2}{24}D_y^2\right)T_{i,j+1/2,k} + O(h^4),$$

$$(3.26)$$

$$\left(\frac{\partial_x T}{f}\right)_{i+1/2,j,k} = \frac{1}{f_0 + \beta y_j}D_x\left(1 - \frac{h^2}{24}D_x^2\right)T_{i+1/2,j,k} + O(h^4).$$

The combination of Eqs. (3.24), (3.25) and (3.26) results in a fourth-order difference equation

$$(D_z u)_{i,j+1/2,k} = \xi_{i,j+1/2,k} \equiv -\left(1 + \frac{\Delta z^2}{24} D_z^2\right) \frac{1}{f_0 + \beta y_{j+1/2}} D_y$$

$$\times \left(1 - \frac{h^2}{24} D_y^2\right) T_{i,j+1/2,k}, \tag{3.27}$$

$$(D_z v)_{i+1/2,j,k} = \zeta_{i+1/2,j,k} \equiv \left(1 + \frac{\Delta z^2}{24} D_z^2\right) \frac{1}{f_0 + \beta y_j} D_x$$

$$\times \left(1 - \frac{h^2}{24} D_x^2\right) T_{i+1/2,j,k}. \tag{3.28}$$

Note that Eqs. (3.27) and (3.28) are evaluated at $z_k$, $1 \leq k \leq N_z - 1$.

Moreover, constraints (2.7b) and (2.8), which state that the vertical average of the horizontal velocity field vanishes everywhere on the horizontal plane (if the homogeneous forcing term $F$ is not present), need to be implemented by a fourth-order integration operator over a staggered grid. For any variable $g$ located at $z_{k+1/2}$ (in the vertical direction), the following integral using a corrected trapezoid rule over a staggered grid is introduced

$$\overline{g}^{**} \equiv \frac{1}{H_0} \left( \sum_{k=0}^{N_z-1} \Delta z \, g_{k+1/2} + \frac{\Delta z}{24} (g_{N+1/2} - g_{N-1/2} - g_{1/2} + g_{-1/2}) \right)$$

$$= \frac{1}{H_0} \int_{-H_0}^{0} g \, dz + O(h^4), \tag{3.29}$$

in which the fourth-order accuracy can be verified through a local Taylor expansion of $g$ over each sub-interval $(z_k, z_{k+1})$, $0 \leq k \leq N_z - 1$. As a result, a fourth-order approximation of Eqs. (2.7b) and (2.8) becomes

$$\overline{u}^{**} \equiv \frac{1}{H_0} \left( \sum_{k=0}^{N_z-1} \Delta z \, u_{k+1/2} + \frac{\Delta z}{24} (u_{N+1/2} - u_{N-1/2} - u_{1/2} + u_{-1/2}) \right) = 0,$$

$$\tag{3.30}$$

$$\overline{v}^{**} \equiv \frac{1}{H_0} \left( \sum_{k=0}^{N_z-1} \Delta z \, v_{k+1/2} + \frac{\Delta z}{24} (v_{N+1/2} - v_{N-1/2} - v_{1/2} + v_{-1/2}) \right) = 0,$$

in which the terms are evaluated at $(i, j + 1/2)$, $(i + 1/2, j)$, respectively. Note that $\frac{\Delta z}{24}(g_{N+1/2} - g_{N-1/2} - g_{1/2} + g_{-1/2})$ is a higher order correction term analogous to the standard second-order integral operator $\overline{g}^* = \frac{1}{H_0} \sum_{k=0}^{N_z-1} \Delta z \, g_{k+1/2} = \frac{1}{H_0} \int_{-H_0}^{0} g \, dz + O(h^2)$. For the horizontal velocity field, such a high-order correction

term can be easily handled by geostrophic balance. On the bottom boundary, a careful calculation indicates

$$(D_z u)_{i,j+1/2,0} = \partial_z u_{i,j+1/2,0} + O(h^2),$$

i.e. ,
$$\frac{u_{i,j+1/2,1/2} - u_{i,j+1/2,-1/2}}{\Delta z} = \frac{-(\partial_y T)_{i,j+1/2,0}}{f_0 + \beta y_{j+1/2}} + O(h^2) \quad (3.31)$$

$$= \frac{-D_y T_{i,j+1/2,0}}{f_0 + \beta y_{j+1/2}} + O(h^2),$$

which in turn shows that

$$u_{i,j+1/2,1/2} - u_{i,j+1/2,-1/2} = -\Delta z \frac{D_y T_{i,j+1/2,0}}{f_0 + \beta y_{j+1/2}} + O(h^3). \quad (3.32)$$

On the top boundary, the estimate turns out to be

$$u_{i,j+1/2,N+1/2} - u_{i,j+1/2,N-1/2} = -\Delta z \frac{D_y T_{i,j+1/2,N}}{f_0 + \beta y_{j+1/2}} + O(h^3). \quad (3.33)$$

The substitution of Eqs. (3.32) and (3.33) into Eq. (3.30) gives

$$\bar{u}_{i,j+1/2}^{**} = \frac{1}{H_0} \left[ \sum_{k=0}^{N_z-1} \Delta z\, u_{i,j+1/2,k+1/2} + \frac{\Delta z^2}{24} \frac{1}{f_0 + \beta y_{j+1/2}} \right.$$

$$\left. \times \left( -D_y T_{i,j+1/2,N} + D_y T_{i,j+1/2,0} \right) \right] + O(h^4). \quad (3.34)$$

Similarly, we have (the details are omitted)

$$\bar{v}_{i+1/2,j}^{**} = \frac{1}{H_0} \left[ \sum_{k=0}^{N_z-1} \Delta z\, v_{i+1/2,j,k+1/2} + \frac{\Delta z^2}{24} \frac{1}{f_0 + \beta y_j} \right.$$

$$\left. \times \left( D_x T_{i+1/2,j,N} - D_x T_{i+1/2,j,0} \right) \right] + O(h^4). \quad (3.35)$$

Therefore, a fourth-order solver to the constraint (3.30)) can be obtained

$$
\begin{aligned}
\sum_{k=0}^{N_z-1} \Delta z\, u_{i,j+1/2,k+1/2} &\equiv CRU_{i,j+1/2} = -\frac{\Delta z^2}{24} \frac{1}{f_0 + \beta y_{j+1/2}} \\
&\times \left(-D_y T_{i,j+1/2,N} + D_y T_{i,j+1/2,0}\right), \\
\sum_{k=0}^{N_z-1} \Delta z\, v_{i+1/2,j,k+1/2} &\equiv CRV_{i+1/2,j} = -\frac{\Delta z^2}{24} \frac{1}{f_0 + \beta y_j} \\
&\times \left(D_x T_{i+1/2,j,N} - D_x T_{i+1/2,j,0}\right).
\end{aligned}
\tag{3.36}
$$

The combination of Eqs. (3.27), (3.28) and (3.36) forms a linear system for the numerical values of the horizontal velocity field, which is composed of $N_z$ unknowns and $N_z$ equations for each component at each fixed horizontal point. The difference equations (3.27) and (3.28) indicate the introduction of (with $\xi$, $\zeta$ given by Eqs. (3.27) and (3.28)

$$
\mathcal{U}_{i,j+1/2,1/2} = 0, \quad \mathcal{U}_{i,j+1/2,k+1/2} = \mathcal{U}_{i,j+1/2,k-1/2} + \Delta z\, \xi_{i,j+1/2,k},
$$
$$
\text{for } 1 \le k \le N_z - 1, \tag{3.37}
$$
$$
\mathcal{V}_{i+1/2,j,1/2} = 0, \quad \mathcal{V}_{i+1/2,j,k+1/2} = \mathcal{V}_{i+1/2,j,k-1/2} + \Delta z\, \zeta_{i+1/2,j,k},
$$
$$
\text{for } 1 \le k \le N_z - 1, \tag{3.38}
$$

so that the differences between $(\mathcal{U}, \mathcal{V})$ and $(u, v)$ are constants. Using the constraint (3.36), we arrive at

$$
u_{i,j+1/2,k+1/2} = \mathcal{U}_{i,j+1/2,k+1/2} - \overline{\mathcal{U}}^*_{i,j+1/2} + \frac{1}{H_0} CRU_{i,j+1/2},
$$
$$
v_{i+1/2,j,k+1/2} = \mathcal{V}_{i+1/2,j,k+1/2} - \overline{\mathcal{V}}^*_{i+1/2,j} + \frac{1}{H_0} CRV_{i+1/2,j}, \tag{3.39}
$$

where $CRU$ and $CRV$ were defined in Eq. (3.36).

### 3.3 Recovery of the vertical velocity field

A fourth-order finite difference method using a mixed approach is applied to Eq. (2.13c) for the determination of the vertical velocity $w$ located at $(i + 1/2, j + 1/2, k)$. A compact operator is used to approximate the derivative $\partial_z^2$

$$
\partial_z^2 = \frac{D_z^2}{1 + \frac{\Delta z^2}{12} D_z^2} + O(h^4). \tag{3.40}
$$

Meanwhile, due to the staggered location in the $x$ direction between $T$ and $w$, the source term $\beta T_x / (f_0 + \beta y)^2$ should be approximated by the long stencil difference (3.4) to facilitate the calculation. Furthermore, to ensure the divergence-free property

of the velocity field at the weakly discrete level as stated below, we choose the source term as

$$
\begin{aligned}
\mathcal{FW} = \frac{\beta}{f_0 + \beta y_{j+1/2}} \cdot \Bigg( & -\frac{1}{16} \frac{1}{f_0 + \beta y_{j-1}} D_x \left(1 - \frac{h^2}{24} D_x^2\right) T_{i+1/2,j-1,k} \\
& + \frac{9}{16} \frac{1}{f_0 + \beta y_j} D_x \left(1 - \frac{h^2}{24} D_x^2\right) T_{i+1/2,j,k} \\
& + \frac{9}{16} \frac{1}{f_0 + \beta y_{j+1}} D_x \left(1 - \frac{h^2}{24} D_x^2\right) T_{i+1/2,j+1,k} \\
& - \frac{1}{16} \frac{1}{f_0 + \beta y_{j+2}} D_x \left(1 - \frac{h^2}{24} D_x^2\right) T_{i+1/2,j+2,k} \Bigg),
\end{aligned}
\tag{3.41}
$$

which is an $O(h^4)$ estimate of the source term evaluated at the grid point $(i + 1/2, j + 1/2, k)$ as shown by a careful analysis. The combination of Eqs. (3.40) and (3.41) leads to the following scheme for the vertical velocity

$$
\begin{cases}
D_z^2 w_{i+1/2,j+1/2,k} = \left(1 + \frac{\Delta z^2}{12} D_z^2\right) \mathcal{FW}_{i+1/2,j+1/2,k}, \\
w_{i+1/2,j+1/2,0} = w_{i+1/2,j+1/2,N_z} = 0.
\end{cases}
\tag{3.42}
$$

At each fixed horizontal grid point $(i + 1/2, j + 1/2)$, the difference equation (3.42) can be easily solved by the FFT-based method in which only the Sine transformation is needed, due to the Dirichlet boundary condition.

## 3.4 Divergence-free property for the numerical velocity field in a weaker sense

As mentioned earlier, the reason for the choice of the source term (3.41) in the determination of the vertical velocity is to guarantee the calculated velocity field to be divergence-free at the discrete level. However, due to the compact operators used in the recovery procedure for both horizontal and vertical velocities, (namely, Eq. (3.25) and (3.40)), a direct verification is not valid. We need to extend the incompressibility constraint $\nabla \cdot \boldsymbol{v} + \partial_z w = 0$ to a generalized form

$$
\nabla \cdot \boldsymbol{v}_z + \partial_z^2 w = 0.
\tag{3.43}
$$

The key point in this subsection is the following proposition, which is a verification of Eq. (3.43) at the discrete level.

**Proposition 3.1** *The numerical velocity determined by the fourth-order scheme satisfies, at the grid point $(i + 1/2, j + 1/2, k)$,*

$$
D_x \left(1 - \frac{h^2}{24} D_x^2\right) \frac{D_z}{1 + \frac{\Delta z^2}{24} D_z^2} u + D_y \left(1 - \frac{h^2}{24} D_y^2\right) \frac{D_z}{1 + \frac{\Delta z^2}{24} D_z^2} v + \frac{D_z^2}{1 + \frac{\Delta z^2}{12} D_z^2} w = 0,
\tag{3.44a}
$$

or equivalently,

$$
D_x \left(1 - \frac{h^2}{24} D_x^2\right) D_z \left(1 + \frac{\Delta z^2}{12} D_z^2\right) u + D_y \left(1 - \frac{h^2}{24} D_y^2\right)
$$
$$
\times D_z \left(1 + \frac{\Delta z^2}{12} D_z^2\right) v + D_z^2 \left(1 + \frac{\Delta z^2}{24} D_z^2\right) w = 0. \qquad (3.44b)
$$

*Proof* We note that all three terms are evaluated at the mesh point $(i+1/2, j+1/2, k)$. The following identity is obtained by using the difference equations (3.27) and (3.28), from which $v$ is recovered

$$
D_x \left(1 - \frac{h^2}{24} D_x^2\right) \frac{D_z}{1 + \frac{\Delta z^2}{24} D_z^2} u
$$
$$
= -\frac{1}{f_0 + \beta y_{j+1/2}} \cdot D_y \left(1 - \frac{h^2}{24} D_y^2\right) \left[D_x \left(1 - \frac{h^2}{24} D_x^2\right) T\right]
$$
$$
= -\frac{1}{f_0 + \beta y_{j+1/2}} \cdot \frac{1}{24\Delta y} \left(D_x \left(1 - \frac{h^2}{24} D_x^2\right) T_{i+1/2, j-1, k} - 27 D_x \left(1 - \frac{h^2}{24} D_x^2\right)\right.
$$
$$
\left. \times T_{i+1/2, j, k} + 27 D_x \left(1 - \frac{h^2}{24} D_x^2\right) T_{i+1/2, j+1, k} - D_x \left(1 - \frac{h^2}{24} D_x^2\right) T_{i+1/2, j+2, k}\right).
$$
$$
(3.45)
$$

We note that the operators in the $x$, $y$, $z$ directions commute. Regarding the second term, a similar reformulation is given by

$$
D_y \left(1 - \frac{h^2}{24} D_y^2\right) \frac{D_z}{1 + \frac{\Delta z^2}{24} D_z^2} v = D_y \left(1 - \frac{h^2}{24} D_y^2\right) \left[\frac{1}{f_0 + \beta y_j} \cdot D_x \left(1 - \frac{h^2}{24} D_x^2\right) T\right]
$$
$$
= \frac{1}{24\Delta y} \left(\frac{1}{f_0 + \beta y_{j-1}} \cdot D_x \left(1 - \frac{h^2}{24} D_x^2\right) T_{i+1/2, j-1, k}\right.
$$
$$
- \frac{27}{f_0 + \beta y_j} \cdot D_x \left(1 - \frac{h^2}{24} D_x^2\right) T_{i+1/2, j, k}
$$
$$
+ \frac{27}{f_0 + \beta y_{j+1}} \cdot D_x \left(1 - \frac{h^2}{24} D_x^2\right) T_{i+1/2, j+1, k}
$$
$$
\left. - \frac{1}{f_0 + \beta y_{j+2}} \cdot D_x \left(1 - \frac{h^2}{24} D_x^2\right) T_{i+1/2, j+2, k}\right). \qquad (3.46)
$$

A careful calculation shows that

$$
D_x \left(1 - \frac{h^2}{24} D_x^2\right) \frac{D_z}{1 + \frac{\Delta z^2}{24} D_z^2} u + D_y \left(1 - \frac{h^2}{24} D_y^2\right) \frac{D_z}{1 + \frac{\Delta z^2}{24} D_z^2} v = -\mathcal{F}\mathcal{W},
$$
$$
(3.47)
$$

in which $\mathcal{FW}$ was defined in Eq. (3.41). The substitution of the difference equation (3.42) into Eq. (3.47) leads to exactly Eq. (3.44a). The identity (3.44b) is a direct consequence of Eq. (3.44a), after multiplication by the operator $\left(1 + \frac{\Delta z^2}{12} D_z^2\right)\left(1 + \frac{\Delta z^2}{24} D_z^2\right)$. Proposition 3.1 is proven. $\qquad\square$

We note that Eq. (3.44a) is a fourth-order discrete approximation of Eq. (3.43), yet it is not convenient to enforce. The equivalent form (3.44b) is easy to check numerically, yet its left side is an $O(h^2)$ discretization of $\nabla \cdot \boldsymbol{v} + \partial_z^2 w$, (more precisely, an $O(h^4)$ discretization of $\left(1 + \frac{\Delta z^2}{12} D_z^2\right)\left(1 + \frac{\Delta z^2}{24} D_z^2\right)\left(\nabla \cdot \boldsymbol{v} + \partial_z^2 w\right)$ ). In our numerical experiment, we observed that Eq. (3.44b) is satisfied at every numerical grid point $(i + 1/2, j + 1/2, k)$ up to a machine error.

Because of the complexity of 3-D flows, it is usually very difficult to prove uniform convergence of fourth-order schemes with physical boundary conditions, especially if an inviscid balance equation is involved. The appropriate usage of both the long-stencil and compact operators, along with the high-order one-sided extrapolation around the boundary, makes the scheme very efficient to implement and enables us to provide a relatively simple convergence analysis under mild regularity assumptions. The following is the main result in this article. Its proof will be provided in Sect. 5.

**Theorem 3.2** *Let* $\boldsymbol{u}_e = (\boldsymbol{v}_e, w_e) \in L^\infty([0, t_1]; C^{8,\alpha})$, $T_e \in L^\infty([0, t_1]; C^{9,\alpha})$ *be the exact solution of the PGEs (2.13), let* $(\boldsymbol{v}_h, w_h, T_h)$ *be the numerical solution of method of lines using the fourth-order method with the MAC grid as described above. Then the following convergence result holds*

$$\|T_e - T_h\|_{L^\infty(0,t_1;L^2)} \leq Ch^4, \tag{3.48a}$$

*where the constant C depends only on the regularity of the exact solution and on the data:*

$$C = C\left(\|T_e\|_{L^\infty(0,t_1;C^{9,\alpha})}, \kappa_1, \kappa_2\right). \tag{3.48b}$$

Note that the exact solution $T_e$ is defined on $[0, t_1] \times \mathcal{M}$, while the numerical solution $T_h$ is defined only on the grid points for $t \in [0, t_1]$.

## 3.5 Temporal discretization

At each time step (stage), the temperature variable is temporally updated at regular numerical grids. Explicit treatment of the nonlinear convection, along with either implicit or explicit time stepping for the temperature diffusion terms, is utilized. Afterward, the velocity field located at the staggered grids is solved via the temperature data by using the methodology outlined above. This approach dramatically simplifies the computation.

The Crank–Nicholson method is chosen as the example of an implicit scheme for the diffusion terms. The classical fourth-order Runge-Kutta method, a multi-stage explicit time stepping procedure, is chosen as a fully explicit scheme. Such an explicit

treatment makes the whole scheme efficient and avoids stability concerns caused by the cell-Reynolds number constraint, especially for high Reynolds number flows.

Given the temperature field $T^n_{i,j,k}$, $1 \leq i, j \leq N - 1$, $0 \leq k \leq N$, we update all the profiles at the time step $t^{n+1}$ through the following procedure.

*Step 1* Temporal evolution of the temperature

**Crank–Nicholson Method** The semi-implicit scheme for the temperature transport equation is given by

$$\frac{T^{n+1} - T^n}{\Delta t} + RHS1^{n+\frac{1}{2}} = \frac{1}{2} \left( \kappa_1 \left( D_x^2 - \frac{h^2}{12} D_x^4 + D_y^2 - \frac{h^2}{12} D_y^4 \right) \right.$$
$$\left. + \kappa_2 \left( D_z^2 - \frac{h^2}{12} D_z^4 \right) \right) \left( T^n + T^{n+1} \right), \quad (3.49a)$$

in which the nonlinear convection term is calculated by a second-order Adams-Basfrod approximation

$$RHS1^{n+\frac{1}{2}}_{i,j,k} = \frac{3}{2} \mathcal{N}_h(\boldsymbol{u}^n, T^n)_{i,j,k} - \frac{1}{2} \mathcal{N}_h(\boldsymbol{u}^{n-1}, T^{n-1})_{i,j,k}. \quad (3.49b)$$

Note that the scheme (3.49) is composed of one Poisson-like equation for $T^{n+1}$ with the prescribed boundary condition (3.15), along with the one-sided extrapolations (3.12), (3.22) and (3.23) at the "ghost" computational points, since long-stencil operators appear. Some fast Poisson solver, such as the FFT-based method, can be applied to facilitate the computation. A mixture of Cosine and Sine transformations are needed in the FFT-based solution due to the boundary condition for $T^{n+1}$.

**RK4 Method** For simplicity, we only present the forward Euler time-discretization. Its extension to the RK4 method is straightforward. At each time step (stage), we update $\left\{ T^{n+1}_{i,j,k} \right\}$, at $(x_i, y_j, z_k)$, for $1 \leq i, j \leq N - 1$, $0 \leq k \leq N$, by

$$\frac{T^{n+1} - T^n}{\Delta t} + \mathcal{N}_h(\boldsymbol{u}^n, T^n)$$
$$= \left( \kappa_1 \left( D_x^2 - \frac{h^2}{12} D_x^4 + D_y^2 - \frac{h^2}{12} D_y^4 \right) + \kappa_2 \left( D_z^2 - \frac{h^2}{12} D_z^4 \right) \right) T^n. \quad (3.50)$$

The same extrapolation formulas for $T$ at "ghost" points are used.

*Step 2* Solve for the horizontal velocity field

With the data of $T^{n+1}$ at hand, which are updated by either Eq. (3.49) or (3.50), we are able to solve for the horizontal velocity field at $t^{n+1}$ via the following system

$$\begin{cases} (D_z u^{n+1})_{i,j+1/2,k} \equiv \xi^{n+1}_{i,j+1/2,k} = -\left(1 + \tfrac{\Delta z^2}{24} D_z^2\right) \tfrac{1}{f_0 + \beta y_{j+1/2}} \\ \qquad\qquad\qquad\qquad\quad \times D_y \left(1 - \tfrac{h^2}{24} D_y^2\right) T^{n+1}_{i,j+1/2,k}, \\ (D_z v^{n+1})_{i+1/2,j,k} \equiv \zeta^{n+1}_{i+1/2,j,k} = \left(1 + \tfrac{\Delta z^2}{24} D_z^2\right) \tfrac{1}{f_0 + \beta y_j} \\ \qquad\qquad\qquad\qquad\quad \times D_x \left(1 - \tfrac{h^2}{24} D_x^2\right) T^{n+1}_{i+1/2,j,k}, \\ \overline{u^{n+1}}^{**}_{i,j+1/2} = 0, \quad \overline{v^{n+1}}^{**}_{i+1/2,j} = 0, \end{cases} \qquad (3.51)$$

which is analogous to Eqs. (3.27), (3.28) and (3.30). The recovery procedure (3.37)–(3.39) can be applied.

*Step 3* Solve for the vertical velocity

We recover the vertical velocity field $w^{n+1}$ as the solution of the following linear system

$$\begin{cases} D_z^2 w^{n+1}_{i+1/2,j+1/2,k} = \left(1 + \tfrac{\Delta z^2}{12} D_z^2\right) \mathcal{F}W^{n+1}_{i+1/2,j+1/2,k}, \\ w^{n+1}_{i+1/2,j+1/2,0} = w^{n+1}_{i+1/2,j+1/2,N_z} = 0. \end{cases} \qquad (3.52)$$

with $\mathcal{F}W$ given by Eq. (3.41).

## 4 Numerical accuracy check

In this section we give an accuracy check for the proposed fourth-order scheme of the PGEs in the alternate formulation. The computational domain is $\mathcal{M} = \mathcal{M}_0 \times [-H_0, 0]$, where $\mathcal{M}_0 = [0, 1]^2$ and $H_0 = 1$. The Coriolis force parameters are given by $f_0 = 1$, $\beta = 1$. The exact temperature function is set to be

$$T_e(x, y, z, t) = \frac{1}{\pi^2} \sin(\pi x)\sin(\pi y)\cos(\pi z)\cos t, \qquad (4.1)$$

so that there is no heat flux at $z = 0, -H_0$ and the temperature vanishes on the four lateral boundary sections. The corresponding exact horizontal velocity $v_e = (u_e, v_e)$ and the vertical velocity $w_e$ are determined by the geostrophic balance and incompressibility condition as formulated in Eqs. (2.13b) and (2.13c), respectively,

$$\begin{cases} \partial_z u_e = -\frac{\partial_y T_e}{f_0 + \beta y} = -\frac{1}{\pi} \frac{1}{1+y} \sin(\pi x)\cos(\pi y)\cos(\pi z)\cos(t), \\ \overline{u_e}(x, y) = 0, \end{cases} \qquad (4.2a)$$

$$\begin{cases} \partial_z v_e = \frac{\partial_x T_e}{f_0 + \beta y} = \frac{1}{\pi} \frac{1}{1+y} \cos(\pi x)\sin(\pi y)\cos(\pi z)\cos(t), \\ \overline{v_e}(x, y) = 0, \end{cases} \qquad (4.2b)$$

$$\begin{cases} \partial_z^2 w_e = \frac{\beta T_x}{(f_0 + \beta y)^2} = \frac{1}{\pi} \frac{1}{(1+y)^2} \cos(\pi x) \sin(\pi y) \cos(\pi z) \cos(t), \\ w_e = 0, \quad \text{at} \quad z = 0, -1. \end{cases} \tag{4.3}$$

The solutions of Eqs. (4.2) and (4.3) turn out to be

$$u_e(x, y, z, t) = -\frac{1}{\pi} \frac{1}{1+y} \sin(\pi x) \cos(\pi y) \left( \frac{1}{\pi} \sin(\pi z) + \frac{2}{\pi^2} \right) \cos(t),$$

$$v_e(x, y, z, t) = \frac{1}{\pi} \frac{1}{1+y} \cos(\pi x) \sin(\pi y) \left( \frac{1}{\pi} \sin(\pi z) + \frac{2}{\pi^2} \right) \cos(t), \tag{4.4}$$

$$w_e(x, y, z, t) = \frac{1}{\pi} \frac{1}{(1+y)^2} \cos(\pi x) \sin(\pi y) \left( -\frac{1}{\pi^2} \cos(\pi z) + \frac{2}{\pi^2} z + \frac{1}{\pi^2} \right) \cos(t).$$

It can be observed that the exact pressure field in the original formulation can be calculated as

$$p_e(x, y, z, t) = \frac{1}{\pi^2} \sin(\pi x) \sin(\pi y) \left( \frac{1}{\pi} \sin(\pi z) + \frac{2}{\pi^2} \right) \cos t, \tag{4.5}$$

so that both the hydrostatic balance $\partial p_e / \partial z = T_e$ and the geostrophic balance $fk \times v_e + \nabla p_e = 0$ are satisfied.

Then we arrive at the following system of PGEs in the alternate formulation (2.13), with the forcing term $f$ added in the temperature transport equation

$$\begin{cases} \partial_t T_e + (v_e \cdot \nabla) T_e + w_e \frac{\partial T_e}{\partial z} = \left( \kappa_1 \Delta + \kappa_2 \partial_z^2 \right) T_e + f, \\ \frac{\partial T_e}{\partial z} = 0, \quad \frac{\partial T_e}{\partial z} = 0, \quad \text{at } z = 0, -H_0, \\ T_e = 0, \quad \text{on } \partial \mathcal{M}_0 \times [-H_0, 0], \end{cases} \tag{4.6a}$$

$$\begin{cases} \partial_z u_e = -\frac{\partial_y T_e}{f_0 + \beta y}, \quad \partial_z v_e = \frac{\partial_x T_e}{f_0 + \beta y}, \\ \overline{u_e}(x, y) = \overline{v_e}(x, y) = 0, \end{cases} \tag{4.6b}$$

$$\begin{cases} \partial_z^2 w_e = \frac{\beta \partial_x T_e}{(f_0 + \beta y)^2}, \\ w_e = 0, \quad \text{at} \quad z = 0, -H_0. \end{cases} \tag{4.6c}$$

The fourth-order method described in Sect. 3, along with the explicit time stepping utilizing the classical RK4 can be used to solve the system (4.6) with the forcing term $f$. Table 1 lists the absolute errors between the numerical and exact solutions for the velocity and temperature. As shown in the table, exact fourth-order accuracy in both the $L^1, L^2$ and $L^\infty$ norms are obtained for the velocity field $u$ and the temperature field. The velocities $v$ and $w$ receive almost fourth-order accuracy in the $L^1$ and $L^2$ norms and slightly less than fourth-order accuracy in the $L^\infty$ norm. The corresponding order of accuracy in the $L^\infty$ norm approaches 4 as the grid is refined. It can be observed that the proposed fourth-order scheme indeed gives an almost exact fourth-order accuracy for all the variables.

**Table 1** Error and order of accuracy for velocity and temperature of the PGEs at $t = 2$ when the fourth-order scheme on staggered grid combined with classical RK4 time stepping are used. We take $\triangle t = 0.4 \triangle x$

|   | $N$ | $L^1$ error | $L^1$ order | $L^2$ error | $L^2$ order | $L^\infty$ error | $L^\infty$ order |
|---|-----|------------|-------------|-------------|-------------|------------------|------------------|
| $u$ | 16 | 1.85e−08 | | 2.62e−08 | | 7.97e−08 | |
| | 32 | 1.16e−09 | 3.99 | 1.65e−09 | 3.99 | 5.01e−09 | 3.99 |
| | 64 | 7.24e−11 | 4.00 | 1.03e−10 | 4.00 | 3.14e−10 | 4.00 |
| | 128 | 4.52e−12 | 4.00 | 6.43e−12 | 4.00 | 1.96e−11 | 4.00 |
| $v$ | 16 | 1.84e−08 | | 2.70e−08 | | 1.23e−07 | |
| | 32 | 1.17e−09 | 3.98 | 1.73e−09 | 3.96 | 8.18e−09 | 3.91 |
| | 64 | 7.41e−11 | 3.98 | 1.10e−10 | 3.98 | 5.24e−10 | 3.96 |
| | 128 | 4.65e−12 | 3.99 | 6.89e−12 | 4.00 | 3.31e−11 | 3.98 |
| $w$ | 16 | 8.09e−09 | | 1.12e−08 | | 2.94e−08 | |
| | 32 | 5.13e−10 | 3.98 | 6.99e−10 | 4.00 | 1.88e−09 | 3.97 |
| | 64 | 3.22e−11 | 3.99 | 4.37e−11 | 4.00 | 1.18e−10 | 3.99 |
| | 128 | 2.01e−12 | 4.00 | 2.73e−12 | 4.00 | 7.36e−12 | 4.00 |
| $T$ | 16 | 2.25e−08 | | 3.35e−08 | | 1.16e−07 | |
| | 32 | 1.42e−09 | 3.99 | 2.09e−09 | 4.00 | 7.20e−09 | 4.00 |
| | 64 | 8.87e−11 | 4.00 | 1.30e−10 | 4.00 | 4.50e−10 | 4.00 |
| | 128 | 5.54e−12 | 4.00 | 8.11e−12 | 4.00 | 2.81e−11 | 4.00 |

## 5 Proof of the fourth-order convergence for smooth solutions

The convergence proof of Theorem 3.2 is composed of a technical consistency analysis for the approximate solutions and the corresponding error estimate. A typical difficulty arises in the analysis of finite difference methods, if a direct truncation error estimate is performed, due to the loss of accuracy near the boundary by a formal observation. To obtain the full accuracy estimate, some cancellation methodology in the approximation must be explored. Instead of substituting the exact solution into the numerical scheme, a careful construction of an approximate temperature profile is performed by adding an $O(h^4)$ correction term to the exact solution to satisfy the full fourth-order truncation error. The approximate velocities (both horizontal and vertical) are given by the numerical recovery solver presented in Sect. 3. Both the approximate temperature and the velocity are shown to be within $O(h^4)$ difference in the $W^{2,\infty}$ and $L^\infty$ norms, respectively. That gives an $O(h^4)$ consistency of the constructed variables. The analysis of the error functions is implemented by the energy estimate of the temperature error equation. It is noted that both the second and fourth-order difference operators appearing in the long-stencil Laplacian operator in Eq. (3.5) are well-posed. This is a crucial fact which leads to the stability of the scheme for the dynamic equation, with a careful treatment of the boundary terms. Furthermore, the $L^2$ norm of the velocity error functions turns out to be bounded by the corresponding norms of the temperature gradient (at the discrete level). This makes the estimate for the nonlinear convection

terms feasible, under an a-priori $L^\infty$ assumption for the error functions, which can be verified by an $O(h^4)$ accuracy in the $L^2$ norm of the temperature.

For simplicity, we set $T^f = 0$ so that the one-sided extrapolation around the top $z = 0$ turns out to be

$$T_{i,j,N+1} = T_{i,j,N-1}, \quad T_{i,j,N+2} = T_{i,j,N-2}, \tag{5.1}$$

by inserting $T^f = 0$. The corresponding extrapolation formulas around $z = -H_0$ and on the four lateral boundary sections are given by Eqs. (3.12), (3.22) and (3.23).

We denote by $T_e$, $\boldsymbol{v}_e$, $w_e$ the exact solution of (2.13), extend $T_e$ smoothly to $[-\delta, 1 + \delta]^2 \times [-H_0 - \delta, \delta]$. To facilitate the analysis of the diffusion term for the temperature, we construct an approximate temperature field $\Theta$ by adding an $O(h^4)$ term to the exact solution $T_e$ to maintain the higher order consistency. In more detail,

$$\Theta = T_e + h^4 \hat{T}, \tag{5.2}$$

in which the correction function $\hat{T}$ satisfies the Poisson equation

$$\triangle \hat{T} = 0, \tag{5.3a}$$

with a mixed-type boundary condition

$$\partial_z \hat{T}(\boldsymbol{x}, -H_0) = \frac{1}{80} \partial_z^5 T_e(\boldsymbol{x}, -H_0), \quad \partial_z \hat{T}(\boldsymbol{x}, 0) = \frac{1}{80} \partial_z^5 T_e(\boldsymbol{x}, 0),$$
$$\hat{T}(0, y, z) = 0, \quad \hat{T}(1, y, z) = 0, \quad \hat{T}(x, 0, z) = 0, \quad \hat{T}(x, 1, z) = 0. \tag{5.3b}$$

Note that $T_e = 0$ on the lateral boundary sections, which implies $\partial_z^5 T_e = 0$ on $\partial\mathcal{M}_0 \times [-H_0, 0]$, hence the difficulty of compatibility at "corner" boundary points is avoided in (5.3). Furthermore, performing a homogenization procedure and applying the Schauder estimate to the above Poisson equation yield

$$\|\hat{T}\|_{C^{m,\alpha}} \leq C \|T_e\|_{C^{m+5,\alpha}}, \quad \text{for } m \geq 2. \tag{5.4}$$

The choice of the Neumann boundary condition for $\hat{T}$ at $z = 0, -H_0$ in Eq. (5.3b) is explained below. We concentrate on the bottom boundary $z = -H_0$. The top boundary can be dealt with in the same way because of the choice $T^f = 0$. A local Taylor expansion for the exact temperature field $T_e$ around the boundary $z = -H_0$ gives

$$(T_e)_{i,j,-1} = (T_e)_{i,j,1} - \frac{h^5}{60} \partial_z^5 T_e(x_i, y_j, -H_0) + O(h^7)\|T_e\|_{C^7},$$

$$(T_e)_{i,j,-2} = (T_e)_{i,j,2} - \frac{32h^5}{60} \partial_z^5 T_e(x_i, y_j, -H_0) + O(h^7)\|T_e\|_{C^7}, \tag{5.5}$$

due to the no-flux boundary condition for $T_e$ and the derivation for $\partial_z^3 T_e$ in Eq. (3.11) by applying the original PDE on the boundary. The substitution of the boundary condition

given by Eq. (5.3b) into the Taylor expansion of $\hat{T}$, along with the Schauder estimate $\|\hat{T}\|_{C^3} \le C\|T_e\|_{C^{8,\alpha}}$ given by Eq. (5.4), leads to

$$
\begin{aligned}
\hat{T}_{i,j,-1} &= \hat{T}_{i,j,1} - 2h\partial_z\hat{T}_{i,j,0} + O(h^3)\partial_z^3\hat{T}_{i,j,0} \\
&= \hat{T}_{i,j,1} - \frac{h}{40}\partial_z^5 T_e(x_i, y_j, -H_0) + O(h^3)\|T_e\|_{C^{8,\alpha}},
\end{aligned}
$$

$$
\begin{aligned}
\hat{T}_{i,j,-2} &= \hat{T}_{i,j,2} - 4h\partial_z\hat{T}_{i,j,0} + O(h^3)\partial_z^3\hat{T}_{i,j,0} \\
&= \hat{T}_{i,j,2} - \frac{h}{20}\partial_z^5 T_e(x_i, y_j, -H_0) + O(h^3)\|T_e\|_{C^{8,\alpha}}.
\end{aligned}
\tag{5.6}
$$

The combination of Eqs. (5.5) and (5.6) results in the following estimate for $\Theta = T_e + h^4\hat{T}$:

$$
\Theta_{i,j,-1} = \Theta_{i,j,1} - \frac{h^5}{24}\partial_z^5 T_e(x_i, y_j, -H_0) + O(h^7)\|T_e\|_{C^{8,\alpha}},
$$

$$
\Theta_{i,j,-2} = \Theta_{i,j,2} - \frac{7h^5}{12}\partial_z^5 T_e(x_i, y_j, -H_0) + O(h^7)\|T_e\|_{C^{8,\alpha}}.
\tag{5.7}
$$

Similar results can be obtained at the top boundary section $z = 0$. It can be seen that the $O(h^5)$ coefficients of $\Theta_{i,j,-1}$, $\Theta_{i,j,-2}$ have the ratio $1 : 14$. This ratio is needed to carry out the error analysis of the inner product of the temperature with its diffusion term. This crucial point is the cause for the choice of the boundary condition for $\hat{T}$ in Eq. (5.3b).

An approximation for $\Theta$ around the lateral boundary sections can be similarly derived. On the left boundary $x = 0$, expansions for $T_e$ and $\hat{T}$ read

$$
(T_e)_{-1,j,k} = \frac{20}{11}(T_e)_{0,j,k} - \frac{6}{11}(T_e)_{1,j,k} - \frac{4}{11}(T_e)_{2,j,k} + \frac{1}{11}(T_e)_{3,j,k} + O(h^5)\|T_e\|_{C^5},
$$

$$
\hat{T}_{-1,j,k} = \frac{20}{11}\hat{T}_{0,j,k} - \frac{6}{11}\hat{T}_{1,j,k} - \frac{4}{11}\hat{T}_{2,j,k} + \frac{1}{11}\hat{T}_{3,j,k} + O(h^2)\|\hat{T}\|_{C^2},
\tag{5.8}
$$

in which the first expansion comes from the derivation (3.22). Applying the Schauder estimate $\|\hat{T}\|_{C^2} \le C\|T_e\|_{C^{7,\alpha}}$ (given by Eq. (5.4)) to Eq. (5.8) results in the extrapolation for $\Theta = T_e + h^4\hat{T}$

$$
\Theta_{-1,j,k} = \frac{20}{11}\Theta_{0,j,k} - \frac{6}{11}\Theta_{1,j,k} - \frac{4}{11}\Theta_{2,j,k} + \frac{1}{11}\Theta_{3,j,k} + O(h^5)\|T_e\|_{C^{7,\alpha}}.
\tag{5.9}
$$

Similar results can be obtained around the three other lateral boundary sections.

One direct consequence of the Schauder estimate (5.4) is

$$
\|\hat{T}\|_{W^{2,\infty}(\mathcal{M})} \le C\|\hat{T}\|_{C^{2,\alpha}} \le C\|T_e\|_{C^{7,\alpha}},
\tag{5.10}
$$

in which $\|\cdot\|_{W^{m,\infty}(\mathcal{M})}$ represents the maximum value at the numerical grids of the given function up to $m$th-order finite-difference, over the 3-D domain $\mathcal{M}$. As a result,

we have

$$\|\Theta - T_e\|_{W^{2,\infty}(\mathcal{M})} = h^4 \|\hat{T}\|_{W^{2,\infty}(\mathcal{M})} \leq C h^4 \|T_e\|_{C^{7,\alpha}}. \tag{5.11}$$

The approximate horizontal velocity $V = (U, V)$ is constructed via the numerical difference scheme given by Eqs. (3.27), (3.28) and (3.36), namely,

$$(D_z U)_{i,j+1/2,k} = -\left(1 + \frac{\Delta z^2}{24} D_z^2\right) \frac{1}{f_0 + \beta y_{j+1/2}} D_y \left(1 - \frac{h^2}{24} D_y^2\right) \Theta_{i,j+1/2,k}, \tag{5.12}$$

$$(D_z V)_{i+1/2,j,k} = \left(1 + \frac{\Delta z^2}{24} D_z^2\right) \frac{1}{f_0 + \beta y_j} D_x \left(1 - \frac{h^2}{24} D_x^2\right) \Theta_{i+1/2,j,k}, \tag{5.13}$$

$$\sum_{k=0}^{N_z-1} \Delta z\, U_{i,j+1/2,k+1/2} = -\frac{\Delta z^2}{24} \frac{1}{f_0 + \beta y_{j+1/2}} \left(-D_y \Theta_{i,j+1/2,N} + D_y \Theta_{i,j+1/2,0}\right),$$

$$\sum_{k=0}^{N_z-1} \Delta z\, V_{i+1/2,j,k+1/2} = -\frac{\Delta z^2}{24} \frac{1}{f_0 + \beta y_j} \left(D_x \Theta_{i+1/2,j,N} - D_x \Theta_{i+1/2,j,0}\right). \tag{5.14}$$

The solver for the linear system (5.12)–(5.14) is analogous to Eqs. (3.37), (3.38) and (3.39). The approximate vertical velocity $W$ is given by the following system at each fixed mesh point $(i + 1/2, j + 1/2)$

$$\begin{cases} D_z^2 W_{i+1/2,j+1/2,k} = \left(1 + \frac{\Delta z^2}{12} D_z^2\right) \mathcal{F}W(\Theta)_{i+1/2,j+1/2,k}, \\ W_{i+1/2,j+1/2,0} = W_{i+1/2,j+1/2,N_z} = 0, \end{cases} \tag{5.15a}$$

in which the force term $\mathcal{F}W(\Theta)$ is defined as

$$\begin{aligned} \mathcal{F}W(\Theta) = \frac{\beta}{f_0 + \beta y_{j+1/2}} \cdot \bigg( & -\frac{1}{16} \frac{1}{f_0 + \beta y_{j-1}} D_x \left(1 - \frac{h^2}{24} D_x^2\right) \Theta_{i+1/2,j-1,k} \\ & + \frac{9}{16} \frac{1}{f_0 + \beta y_j} D_x \left(1 - \frac{h^2}{24} D_x^2\right) \Theta_{i+1/2,j,k} \\ & + \frac{9}{16} \frac{1}{f_0 + \beta y_{j+1}} D_x \left(1 - \frac{h^2}{24} D_x^2\right) \Theta_{i+1/2,j+1,k} \\ & - \frac{1}{16} \frac{1}{f_0 + \beta y_{j+2}} D_x \left(1 - \frac{h^2}{24} D_x^2\right) \Theta_{i+1/2,j+2,k} \bigg). \end{aligned} \tag{5.15b}$$

The estimate for the constructed vertical velocity is given below.

**Proposition 5.1** *We have*

$$\|W - w_e\|_{L^\infty} \leq Ch^4 \|T_e\|_{C^8}. \tag{5.16}$$

*Proof* A detailed calculation of the Taylor expansion for the exact temperature $T_e$ and the vertical velocity $w_e$ gives

$$\left(1 + \frac{\Delta z^2}{12} D_z^2\right) \mathcal{F}\mathcal{W}(T_e)_{i+1/2, j+1/2, k}$$
$$= \left(1 + \frac{\Delta z^2}{12} \partial_z^2\right) \left(\frac{\beta \partial_x T_e}{(f_0 + \beta y)^2}\right)_{i+1/2, j+1/2, k} + O(h^4)\|T_e\|_{C^5}, \tag{5.17}$$

$$D_z^2 w_e = \left(1 + \frac{\Delta z^2}{12} D_z^2\right) \partial_z^2 w_e + O(h^4)\|w_e\|_{C^6} = \left(1 + \frac{\Delta z^2}{12} \partial_z^2\right)$$
$$\times \frac{\beta \partial_x T_e}{(f_0 + \beta y)^2} + O(h^4)\|w_e\|_{C^6}, \text{ at } (i+1/2, j+1/2, k). \tag{5.18}$$

Also, an application of Eq. (5.11) yields

$$\mathcal{F}\mathcal{W}(\Theta) - \mathcal{F}\mathcal{W}(T_e) = \mathcal{F}\mathcal{W}(\Theta - T_e) \leq C\|\Theta - T_e\|_{W^{1,\infty}(\mathcal{M})} \leq Ch^4\|T_e\|_{C^{6,\alpha}}, \tag{5.19}$$

since $\mathcal{F}\mathcal{W}$ is a linear operator which involves only a discrete gradient of temperature. The combination of Eqs. (5.17)–(5.19) leads to the following system

$$\begin{cases} D_z^2(w_e)_{i+1/2, j+1/2, k} = \left(1 + \frac{\Delta z^2}{12} D_z^2\right) \mathcal{F}\mathcal{W}(\Theta)_{i+1/2, j+1/2, k} + h^4 f_w, \\ (w_e)_{i+1/2, j+1/2, 0} = (w_e)_{i+1/2, j+1/2, N_z} = 0, \end{cases} \tag{5.20}$$

in which $f_w \leq C\|T_e\|_{C^8}$. Subtracting Eq. (5.15) from Eq. (5.20) results in

$$\begin{cases} D_z^2(w_e - W)_{i+1/2, j+1/2, k} = h^4 f_w, \\ (w_e - W)_{i+1/2, j+1/2, 0} = (w_e - W)_{i+1/2, j+1/2, N_z} = 0. \end{cases} \tag{5.21}$$

Due to the homogeneous Dirichlet boundary condition for $\tilde{w} = w_e - W$ at $k = 0, N$, we apply the maximum principle to Eq. (5.21) and arrive at

$$\|W - w_e\|_{L^\infty(i+1/2, j+1/2)} \leq C\|D_z^2\tilde{w}\|_{L^\infty(i+1/2, j+1/2)} \leq Ch^4\|T_e\|_{C^6}. \tag{5.22}$$

Note that Eq. (5.22) is valid for each fixed grid $(i + 1/2, j + 1/2)$. Then we arrive at Eq. (5.16). Proposition 5.1 is proven. □

The estimate for the approximate horizontal velocity determined by Eqs. (5.12)–(5.14) comes from the Taylor expansion for $T_e$ and the recovery formulas (3.37)–(3.39). The following results can be obtained

$$\|U - u_e\|_{L^\infty} + \|V - v_e\|_{L^\infty} \le Ch^4\|T_e\|_{C^8}. \tag{5.23}$$

As a result of Eqs. (5.16) and (5.23), we have the following estimate of the averaged velocities at the regular numerical grid points $(i, j, k)$:

$$
\begin{aligned}
\mathcal{A}_y(\mathcal{A}_z U)_{i,j,k} - (u_e)_{i,j,k} &= \mathcal{A}_y(\mathcal{A}_z[U - u_e])_{i,j,k} + \mathcal{A}_y(\mathcal{A}_z u_e)_{i,j,k} - (u_e)_{i,j,k} \\
&= O(h^4)\|T_e\|_{C^8} + O(h^4)\|u_e\|_{C^4} = O(h^4)\|T_e\|_{C^8}, \\
\mathcal{A}_x(\mathcal{A}_z V)_{i,j,k} - (v_e)_{i,j,k} &= O(h^4)\|T_e\|_{C^8}, \\
\mathcal{A}_x(\mathcal{A}_y W)_{i,j,k} - (w_e)_{i,j,k} &= O(h^4)\|T_e\|_{C^8}.
\end{aligned}
\tag{5.24}
$$

The combination of Eqs. (5.11) and (5.24), along with Taylor expansion for $T_e$, leads to

$$
\begin{aligned}
\mathcal{A}_y(\mathcal{A}_z U)\tilde{D}_x \left(1 - \frac{h^2}{6}D_x^2\right)\Theta &= u_e\partial_x T_e + O(h^4)\|T_e\|_{C^8}\|T_e\|_{C^{7,\alpha}}, \\
\mathcal{A}_x(\mathcal{A}_z V)\tilde{D}_y \left(1 - \frac{h^2}{6}D_y^2\right)\Theta &= v_e\partial_y T_e + O(h^4)\|T_e\|_{C^8}\|T_e\|_{C^{7,\alpha}}, \quad (5.25) \\
\mathcal{A}_x(\mathcal{A}_y W)\tilde{D}_y \left(1 - \frac{h^2}{6}D_z^2\right)\Theta &= w_e\partial_z T_e + O(h^4)\|T_e\|_{C^8}\|T_e\|_{C^{7,\alpha}},
\end{aligned}
$$

$$
\begin{aligned}
&\left(\kappa_1\left(D_x^2 - \frac{h^2}{12}D_x^4 + D_y^2 - \frac{h^2}{12}D_y^4\right) + \kappa_2\left(D_z^2 - \frac{h^2}{12}D_z^4\right)\right)\Theta \\
&= (\kappa_1\triangle + \kappa_2\partial_z^2)T_e + O(h^4)\|T_e\|_{C^{7,\alpha}}.
\end{aligned}
\tag{5.26}
$$

Moreover, taking the temporal derivative of (5.3) leads to a Poisson equation for $\partial_t\hat{T}$

$$\triangle(\partial_t\hat{T}) = 0, \tag{5.27a}$$

$$\partial_z(\partial_t\hat{T})(\boldsymbol{x}, -H_0) = \frac{1}{80}(\partial_t\partial_z^5 T_e)(\boldsymbol{x}, -H_0), \quad \partial_z(\partial_t\hat{T})(\boldsymbol{x}, 0) = \frac{1}{80}(\partial_t\partial_z^5 T_e)(\boldsymbol{x}, 0), \tag{5.27b}$$

$$\partial_t\hat{T}(0, y, z) = 0, \quad \partial_t\hat{T}(1, y, z) = 0, \partial_t\hat{T}(x, 0, z) = 0, \quad \partial_t\hat{T}(x, 1, z) = 0.$$

The Schauder estimate applied to the above Poisson equation reads

$$
\begin{aligned}
\|\partial_t\hat{T}\|_{C^{m,\alpha}} &\le C\|\partial_t T_e\|_{C^{m+5,\alpha}} \\
&\le C\left(\|u_e\|_{C^{m+5,\alpha}}\|T_e\|_{C^{m+6,\alpha}} + \|T_e\|_{C^{m+7,\alpha}}\right), \quad \text{for } m \ge 2, \tag{5.28}
\end{aligned}
$$

in which the original temperature transport equation $\partial_t T_e + (\boldsymbol{v} \cdot \nabla) T_e + w_e \partial_z T_e = (\kappa_1 \Delta + \kappa_2 \partial_z^2) T_e$ was used. It can be seen that Eq. (5.28) amounts to saying that

$$\partial_t \Theta = \partial_t T_e + O(h^4) \left( \|T_e\|_{C^{8,\alpha}}^2 + \|T_e\|_{C^{9,\alpha}} \right). \tag{5.29}$$

The combination of Eqs. (5.25), (5.26), (5.29) and the original temperature equation gives

$$\partial_t \Theta + \mathcal{N}_h(\boldsymbol{U}, \Theta) = \left( \kappa_1 \left( D_x^2 - \frac{h^2}{12} D_x^4 + D_y^2 - \frac{h^2}{12} D_y^4 \right) + \kappa_2 \left( D_z^2 - \frac{h^2}{12} D_z^4 \right) \right) \Theta$$
$$+ h^4 \boldsymbol{f}_T, \tag{5.30}$$

where $|\boldsymbol{f}_T| \leq C(\|T_e\|_{C^{8,\alpha}}^2 + \|T_e\|_{C^{9,\alpha}})$.

We define the error functions of the temperature and the velocity at different mesh points by

$$\tilde{T} = \Theta - T, \quad \tilde{\boldsymbol{v}} = (\tilde{u}, \tilde{v}) = (U - u, V - v), \quad \tilde{w} = W - w. \tag{5.31}$$

Subtracting Eqs. (5.30), (5.12)–(5.14) and (5.15) from the numerical scheme (3.5), (3.27), (3.28), (3.36) and (3.42) gives

$$\begin{cases} \partial_t \tilde{T} + \mathcal{N}_h(\tilde{\boldsymbol{u}}, T) + \mathcal{N}_h(\boldsymbol{U}, \tilde{T}) = \left( \kappa_1 \left( D_x^2 - \frac{h^2}{12} D_x^4 + D_y^2 - \frac{h^2}{12} D_y^4 \right) \right. \\ \left. + \kappa_2 \left( D_z^2 - \frac{h^2}{12} D_z^4 \right) \right) \tilde{T} + h^4 \boldsymbol{f}_T, \\ \tilde{T}_{0,j,k} = 0, \quad \tilde{T}_{N,j,k} = 0, \quad \tilde{T}_{i,0,k} = 0, \quad \tilde{T}_{i,N,k} = 0, \end{cases} \tag{5.32a}$$

$$(D_z \tilde{u})_{i,j+1/2,k} = -\left( 1 + \frac{\Delta z^2}{24} D_z^2 \right) \frac{1}{f_0 + \beta y_{j+1/2}} D_y \left( 1 - \frac{h^2}{24} D_y^2 \right) \tilde{T}_{i,j+1/2,k},$$
$$\tag{5.32b}$$
$$(D_z \tilde{v})_{i+1/2,j,k} = \left( 1 + \frac{\Delta z^2}{24} D_z^2 \right) \frac{1}{f_0 + \beta y_j} D_x \left( 1 - \frac{h^2}{24} D_x^2 \right) \tilde{T}_{i+1/2,j,k},$$

$$\sum_{k=0}^{N_z-1} \Delta z \, \tilde{u}_{i,j+1/2,k+1/2} = -\frac{\Delta z^2}{24} \frac{1}{f_0 + \beta y_{j+1/2}} \left( -D_y \tilde{T}_{i,j+1/2,N} + D_y \tilde{T}_{i,j+1/2,0} \right),$$

$$\sum_{k=0}^{N_z-1} \Delta z \, \tilde{v}_{i+1/2,j,k+1/2} = -\frac{\Delta z^2}{24} \frac{1}{f_0 + \beta y_j} \left( D_x \tilde{T}_{i+1/2,j,N} - D_x \tilde{T}_{i+1/2,j,0} \right),$$

$$\begin{cases} D_z^2 \tilde{w}_{i+1/2,j+1/2,k} = \left( 1 + \frac{\Delta z^2}{12} D_z^2 \right) \mathcal{FW}(\tilde{T})_{i+1/2,j+1/2,k}, \\ \tilde{w}_{i+1/2,j+1/2,0} = \tilde{w}_{i+1/2,j+1/2,N_z} = 0. \end{cases} \tag{5.32c}$$

Regarding the "ghost" point values for $\tilde{T}$, we conclude from Eqs. (5.7), (5.9) and (5.11) that

$$\tilde{T}_{i,j,-1} = \tilde{T}_{i,j,1} - \frac{h^5}{24} r_{i,j}^b + h^7 e_{i,j}^{b1}, \quad \tilde{T}_{i,j,-2} = \tilde{T}_{i,j,2} - \frac{7h^5}{12} r_{i,j}^b + h^7 e_{i,j}^{b2},$$

$$\tilde{T}_{-1,j,k} = \frac{20}{11}\tilde{T}_{0,j,k} - \frac{6}{11}\tilde{T}_{1,j,k} - \frac{4}{11}\tilde{T}_{2,j,k} + \frac{1}{11}\tilde{T}_{3,j,k} + h^5 e_{j,k}^{l1}, \tag{5.33a}$$

with

$$r_{i,j}^b = \partial_z^5 T_e(x_i, y_j, -H_0), \quad |e_{i,j}^{b1}|, |e_{i,j}^{b2}| \le C\|T_e\|_{C^{8,\alpha}}, \quad |e_{j,k}^{l1}| \le C\|T_e\|_{C^{7,\alpha}}. \tag{5.33b}$$

Once again, we observe that the $O(h^5)$ coefficients of $\tilde{T}_{i,j,-1}$, $\tilde{T}_{i,j,-2}$ have the ratio $1 : 14$. Such a ratio is crucial to the error analysis of the temperature diffusion term in Eq. (5.32a).

To proceed with the energy estimate of the nonlinear system (5.32), (5.33), we introduce the following notation. For any pair of variables $f$, $g$ which are evaluated at the 3-D regular mesh points $(i, j, k)$, the following discrete $L^2$-inner product are introduced

$$\langle f, g \rangle = \triangle z \left( \frac{1}{2}\langle f, g \rangle_{z0} + \sum_{k=1}^{N-1} \langle f, g \rangle_{zk} + \frac{1}{2}\langle f, g \rangle_{zN} \right),$$

$$\text{with} \quad \langle f, g \rangle_{zk} = h^2 \sum_{j=1}^{N-1} \sum_{i=1}^{N-1} f_{i,j,k}\, g_{i,j,k}. \tag{5.34}$$

The corresponding $L^2$ norm can be defined. In addition, the $L^2$ norm for the discrete temperature gradient is defined as

$$\|\nabla_h \tilde{T}\|_2^2 = \|D_x \tilde{T}\|_2^2 + \|D_y \tilde{T}\|_2^2, \quad \text{with}$$

$$\|D_x \tilde{T}\|_2^2 = \triangle z \left( \frac{1}{2}\|D_x \tilde{T}\|_{z0}^2 + \sum_{k=1}^{N-1} \|D_x \tilde{T}\|_{zk}^2 + \frac{1}{2}\|D_x \tilde{T}\|_{zk}^2 \right),$$

$$\|D_x \tilde{T}\|_{zk}^2 = h^2 \sum_{j=1}^{N-1} \sum_{i=0}^{N-1} (D_x^+ \tilde{T})_{i,j,k}^2,$$

$$\|D_y \tilde{T}\|_2^2 = \triangle z \left( \frac{1}{2}\|D_y \tilde{T}\|_{z0}^2 + \sum_{k=1}^{N-1} \|D_y \tilde{T}\|_{zk}^2 + \frac{1}{2}\|D_y \tilde{T}\|_{zk}^2 \right),$$

$$\|D_y \tilde{T}\|_{zk}^2 = h^2 \sum_{j=1}^{N-1} \sum_{i=0}^{N-1} (D_y^+ \tilde{T})_{i,j,k}^2 \tag{5.35}$$

$$\|D_z \tilde{T}\|_2^2 = h^3 \sum_{j=1}^{N-1} \sum_{i=1}^{N-1} \sum_{k=0}^{N-1} (D_z^+ \tilde{T})_{i,j,k}^2. \tag{5.36}$$

A key point in the stability analysis of the system (5.32) is that the velocity error is bounded by the temperature gradient error in the $L^2$ norm, which comes from a careful analysis of Eqs. (5.32b) and (5.32c). The results are stated below. Its verification is straightforward:

$$\|\mathcal{A}_y(\mathcal{A}_z\tilde{u})\|, \|\mathcal{A}_x(\mathcal{A}_z\tilde{v})\|, \|\mathcal{A}_x(\mathcal{A}_y\tilde{w})\| \leq C_1\|\nabla_h\tilde{T}\|_2. \tag{5.37}$$

Taking the $\langle\ ,\ \rangle$ product of Eq. (5.32a) with $\tilde{T}$ yields (see the definition (5.34))

$$\frac{1}{2}\frac{d}{dt}\|\tilde{T}\|^2 - \kappa_1\left\langle\tilde{T}, \left(\triangle_h - \frac{h^2}{12}(D_x^4 + D_y^4)\right)\tilde{T}\right\rangle - \kappa_2\left\langle\tilde{T}, \left(D_z^2 - \frac{h^2}{12}D_z^4\right)\tilde{T}\right\rangle$$
$$= -\langle\tilde{T}, \mathcal{N}_h(\boldsymbol{U}, \tilde{T})\rangle - \langle\tilde{T}, \mathcal{N}_h(\tilde{\boldsymbol{u}}, T)\rangle + h^4\langle\tilde{T}, \boldsymbol{f}_T\rangle. \tag{5.38}$$

The estimate of the temperature diffusion term is outlined in the next two propositions. Its proof relies on the stability of the long-stencil operator. We note that both the second-order (such as $D_x^2$, $D_y^2$, $D_z^2$) and fourth-order difference operators (such as $D_x^4$, $D_y^4$, $D_z^4$) appearing in the long-stencil Laplacian operator in Eq. (3.5) have negative eigenvalues with respect to either the Dirichlet or Neumann boundary condition. This is the crucial reason for the feasibility of its stability analysis. In addition, a careful treatment of the boundary terms is required to carry out the estimate.

**Proposition 5.2** *We have*

$$-\left\langle\tilde{T}, (D_z^2 - \frac{h^2}{12}D_z^4)\tilde{T}\right\rangle \geq \frac{3}{4}\|D_z\tilde{T}\|_2^2 - \frac{1}{2}h^8 - h^2\|\tilde{T}\|^2. \tag{5.39}$$

*Proof* Summing by parts under the inner product $\langle\ ,\ \rangle$ and using the boundary extrapolation (5.33) give

$$\left\langle\tilde{T}, (D_z^2 - \frac{h^2}{12}D_z^4)\tilde{T}\right\rangle = -\|D_z\tilde{T}\|_2^2 - \frac{h^2}{12}\|D_z^2\tilde{T}\|^2 + \mathcal{B}^{b1} + \mathcal{B}^{b2}, \tag{5.40}$$

in which $\mathcal{B}^{b1}$, corresponding to the boundary term around $z = -H_0$, reads

$$\mathcal{B}^{b1} = \frac{h}{12}\sum_{j=1}^{N-1}\sum_{i=1}^{N-1}\left(\tilde{T}_{i,j,1}\big(\tilde{T}_{i,j,-1} - \tilde{T}_{i,j,1}\big) + \frac{1}{2}\tilde{T}_{i,0}\right.$$
$$\times\left[\big(\tilde{T}_{i,j,-2} - \tilde{T}_{i,j,2}\big) - 16\big(\tilde{T}_{i,j,-1} - \tilde{T}_{i,j,1}\big)\right]\bigg)$$
$$= \frac{h}{12}\sum_{j=1}^{N-1}\sum_{i=1}^{N-1}\left(\tilde{T}_{i,j,1}\left[-\frac{h^5}{24}r_{i,j}^b + h^7e_{i,j}^{b1}\right]\right.$$
$$+ \frac{1}{2}\tilde{T}_{i,j,0}\left[-\frac{7h^5}{12}r_{i,j}^b + e_{i,j}^{b2} - 16\left(-\frac{h^5}{24}r_{i,j}^b + h^7e_{i,j}^{b1}\right)\right]\bigg), \tag{5.41}$$

and $\mathcal{B}^{b2}$ can be similarly given. It should be noted that the derivation of Eq. (5.41) comes from the formula for $\tilde{T}_{i,j,-1}$, $\tilde{T}_{i,j,-2}$ in Eq. (5.33a) and that $r^b$, $e^{b1}$, $e^{b2}$ are given by Eq. (5.33b). More precisely, $\mathcal{B}^{b1}$ can be simplified as

$$
\begin{aligned}
\mathcal{B}^{b1} &= \frac{h^8}{12} \sum_{j=1}^{N-1} \sum_{i=1}^{N-1} \left( e_{i,j}^{b1}(\tilde{T}_{i,j,1} - 8\tilde{T}_{i,j,0}) + \frac{1}{2} e_{i,j}^{b2} \tilde{T}_{i,j,0} \right) \\
&\quad + \frac{h^6}{288} \sum_{j=1}^{N-1} \sum_{i=1}^{N-1} r_{i,j}^b(\tilde{T}_{i,j,0} - \tilde{T}_{i,j,1}) \\
&\equiv I_1^b + I_2^b.
\end{aligned}
\tag{5.42}
$$

The term $I_1^b$ can be controlled by the Cauchy inequality and the estimate (5.33b)

$$
I_1^b \le Ch^8 \left| \sum_{j=1}^{N-1} \sum_{i=1}^{N-1} e_{i,j}^{b1} \tilde{T}_{i,j,1} \right| + Ch^8 \left| \sum_{j=1}^{N-1} \sum_{i=1}^{N-1} e_{i,j}^{b1} \tilde{T}_{i,j,0} \right| \le C\|\tilde{T}\|^2 + Ch^9,
\tag{5.43}
$$

since $e$ is bounded.

What remains is the estimate of $I_2^b$. As can be seen, the detailed estimate for $\tilde{T}_{i,j,-1}$, $\tilde{T}_{i,j,-2}$ in (5.33), which shows that the $O(h^5)$ coefficients of $\tilde{T}_{i,j,-1}$, $\tilde{T}_{i,j,-2}$ have the ratio $1:14$, makes the term $I_2^b$ have the form $\frac{h^6}{288} \sum_{j=1}^{N-1} \sum_{i=1}^{N-1} r_{i,j}^b(\tilde{T}_{i,j,0} - \tilde{T}_{i,j,1})$. That is crucial to the error analysis below. The application of the Cauchy inequality shows that

$$
\begin{aligned}
I_2^b &= \frac{h^6}{288} \sum_{j=1}^{N-1} \sum_{i=1}^{N-1} r_{i,j}^b(\tilde{T}_{i,j,0} - \tilde{T}_{i,j,1}) \\
&\le \frac{1}{288} h^3 \sum_{j=1}^{N-1} \sum_{i=1}^{N-1} \frac{(\tilde{T}_{i,j,0} - \tilde{T}_{i,j,1})^2}{h^2} + \frac{1}{288} h^{11} \sum_{j=1}^{N-1} \sum_{i=1}^{N-1} (r_{i,j}^b)^2. \quad (5.44)
\end{aligned}
$$

It is observed that the first term appearing above can be absorbed into $\|D_z\tilde{T}\|_2^2$. Meanwhile, we note that $r_{i,j}^b = \partial_z^5 T_e(x_i, y_j, -H_0)$ is a bounded quantity. Then we obtain

$$
I_2^b = \frac{h^6}{288} \sum_{j=1}^{N-1} \sum_{i=1}^{N-1} r_{i,j}^b(\tilde{T}_{i,j,0} - \tilde{T}_{i,j,1}) \le \frac{1}{288} \|D_z\tilde{T}\|_2^2 + Ch^9.
\tag{5.45}
$$

The combination of Eqs. (5.43) and (5.45) leads to

$$
\mathcal{B}^{b1} \le \frac{1}{288} \|D_z\tilde{T}\|_2^2 + \frac{1}{8} h^8.
\tag{5.46}
$$

The other boundary term $\mathcal{B}^{b2}$ can be similarly treated. Going back to Eq. (5.40), we obtain the estimate (5.39). Proposition 5.2 is proven. □

**Proposition 5.3** *We have*

$$-\left\langle \tilde{T}, \left(D_x^2 - \frac{h^2}{12}D_x^4\right)\tilde{T}\right\rangle \geq \frac{1}{2}\|D_x\tilde{T}\|_2^2 - h^8. \tag{5.47}$$

*Proof* At each fixed vertical grid point $z_k$, the temperature error $\tilde{T}$ vanishes at $i = 0, N$. As a result, summing by parts gives

$$-\left\langle \tilde{T}, \left(D_x^2 - \frac{h^2}{12}D_x^4\right)\tilde{T}\right\rangle_{zk} = \|D_x\tilde{T}\|_{zk}^2 + \frac{h^2}{12}\|D_x^2\tilde{T}\|_{zk}^2 + \frac{h^2}{12}\mathcal{B}^{l1} + \frac{h^2}{12}\mathcal{B}^{l2}, \tag{5.48}$$

where $\mathcal{B}^{l1}$, $\mathcal{B}^{l2}$ correspond to the boundary terms

$$\mathcal{B}^{l1} = \sum_{j=1}^{N-1} \tilde{T}_{1,j,k}(D_x^2\tilde{T})_{0,j,k}, \quad \mathcal{B}^{l2} = \sum_{j=1}^{N-1} \tilde{T}_{N-1,j,k}(D_x^2\tilde{T})_{N,j,k}. \tag{5.49}$$

By the boundary condition for $\tilde{T}$ at the "ghost points" as in (5.33), $(D_x^2\tilde{T})_{0,j,k}$ can be written as

$$(D_x^2\tilde{T})_{0,j,k} = \frac{1}{h^2}\left(-\frac{2}{11}\tilde{T}_{0,j,k} + \frac{5}{11}\tilde{T}_{1,j,k} - \frac{4}{11}\tilde{T}_{2,j,k} + \frac{1}{11}\tilde{T}_{3,j,k}\right) + h^3 e_{j,k}^{l1}. \tag{5.50}$$

Since $\tilde{T}$ does vanish at $i = 0, N$, Eq. (5.50) can be rewritten as

$$(D_x^2\tilde{T})_{0,j,k} = -\frac{2}{11}(D_x^2\tilde{T})_{1,j,k} + \frac{1}{11}(D_x^2\tilde{T})_{2,j,k} + h^3 e_{j,k}^{l1}. \tag{5.51}$$

The purpose of this transformation is to control local terms by global terms as is shown later. Using the Cauchy inequality for each term appearing in Eq. (5.51) leads to

$$\begin{aligned}
\tilde{T}_{1,j,k}(D_x^2\tilde{T})_{0,j,k} &\geq -\frac{2^2}{4\cdot 11^2\cdot h^2}\tilde{T}_{1,j,k}^2 - h^2(D_x^2\tilde{T}_{1,j,k})^2 - \frac{1^2}{4\cdot 11^2\cdot h^2}\tilde{T}_{1,j,k}^2 \\
&\quad - h^2(D_x^2\tilde{T}_{2,j,k})^2 - \frac{1}{4h^2}\tilde{T}_{1,j,k}^2 - h^8(e_{j,k}^{l1})^2 \\
&\geq -\frac{1}{2h^2}\tilde{T}_{1,j,k}^2 - h^2(D_x^2\tilde{T}_{1,j,k})^2 - h^2(D_x^2\tilde{T}_{2,j,k})^2 - h^8(e_{j,k}^{l1})^2.
\end{aligned} \tag{5.52}$$

The first term appearing above can be controlled by $\|D_x\tilde{T}\|_{zk}^2$, since we will multiply it by $\frac{h^2}{12}$, leaving more than $\frac{1}{2}\|D_x\tilde{T}\|_{zk}^2$; the second and third terms will be controlled

by $\|D_x^2 \tilde{T}\|_{zk}^2$; the last term can be controlled by

$$\frac{h^2}{12} \sum_{j=1}^{N-1} h^8 \left(e_{j,k}^{l1}\right)^2 \leq N h^{10} \cdot C \|T_e\|_{C^{6,\alpha}}^2 \leq C h^9 \|T_e\|_{C^{6,\alpha}}^2, \tag{5.53}$$

where we used the fact that $h = \frac{1}{N}$. Then we arrive at

$$-\left\langle \tilde{T}, \left(D_x^2 - \frac{h^2}{12} D_x^4\right) \tilde{T} \right\rangle_{zk} \geq \frac{1}{2} \|D_x \tilde{T}\|_{zk}^2 - \frac{1}{8} h^8. \tag{5.54}$$

Proposition 5.3 is proven since Eq. (5.54) is valid for each fixed $k$. $\qquad\square$

Similar to Eq. (5.47), we can also obtain

$$-\left\langle \tilde{T}, \left(D_y^2 - \frac{h^2}{12} D_y^4\right) \tilde{T} \right\rangle \geq \frac{1}{2} \|D_y \tilde{T}\|_2^2 - h^8. \tag{5.55}$$

The analysis for the linearized convection terms is given below.

**Proposition 5.4** *Assume a-priori that the error function for the temperature field satisfies*

$$\|\tilde{T}\|_{L^\infty} \leq h^2. \tag{5.56}$$

*Then we have*

$$\left|\langle \tilde{T}, \mathcal{N}_h(\tilde{\boldsymbol{u}}, T)\rangle\right|, \ \left|\langle \tilde{T}, \mathcal{N}_h(\boldsymbol{U}, \tilde{T})\rangle\right| \leq \tilde{C}_1 \|\tilde{T}\|^2 + \frac{\kappa_0}{2} \left(\|\nabla_h \tilde{T}\|_2^2 + \|D_z \tilde{T}\|_2^2\right), \tag{5.57}$$

*with $\kappa_0 = min(\kappa_1, \kappa_2)$ and $\tilde{C}_1 = C\left(\|T_e\|_{C^{9,\alpha}}, \kappa_0\right)$.*

*Proof* By the a-priori bound (5.56) and the estimate (5.11), we have

$$\|\tilde{T}\|_{W^{1,\infty}(\mathcal{M})} \leq Ch, \quad \text{which implies}$$
$$\|T\|_{W^{1,\infty}(\mathcal{M})} \leq \|\Theta\|_{W^{1,\infty}(\mathcal{M})} + \|\tilde{T}\|_{W^{1,\infty}(\mathcal{M})} \leq \|T_e\|_{C^1} + 1. \tag{5.58}$$

This result will be used later. The inner product of $\tilde{T}$ with the linearized convection terms can be decomposed as

$$
\begin{aligned}
\langle \tilde{T}, \mathcal{N}_h(\tilde{\boldsymbol{u}}, T) \rangle &= \left\langle \tilde{T}, \mathcal{A}_y(\mathcal{A}_z \tilde{u})\, \tilde{D}_x \left(1 - \frac{h^2}{6} D_x^2\right) T \right\rangle \\
&\quad + \left\langle \tilde{T}, \mathcal{A}_x(\mathcal{A}_z \tilde{v})\, \tilde{D}_y \left(1 - \frac{h^2}{6} D_y^2\right) T \right\rangle \\
&\quad + \left\langle \tilde{T}, \mathcal{A}_x(\mathcal{A}_y \tilde{w})\, \tilde{D}_z \left(1 - \frac{h^2}{6} D_z^2\right) T \right\rangle, \\
\langle \tilde{T}, \mathcal{N}_h(U, \tilde{T}) \rangle &= \left\langle \tilde{T}, \mathcal{A}_y(\mathcal{A}_z U)\, \tilde{D}_x \left(1 - \frac{h^2}{6} D_x^2\right) \tilde{T} \right\rangle \\
&\quad + \left\langle \tilde{T}, \mathcal{A}_x(\mathcal{A}_z V)\, \tilde{D}_y \left(1 - \frac{h^2}{6} D_y^2\right) \tilde{T} \right\rangle \\
&\quad + \left\langle \tilde{T}, \mathcal{A}_x(\mathcal{A}_y W)\, \tilde{D}_z \left(1 - \frac{h^2}{6} D_z^2\right) \tilde{T} \right\rangle.
\end{aligned}
\tag{5.59}
$$

For the first term appearing in $\langle \tilde{T}, \mathcal{N}_h(\tilde{\boldsymbol{u}}, T) \rangle$, we see that

$$
\begin{aligned}
\left| \left\langle \tilde{T}, \mathcal{A}_y(\mathcal{A}_z \tilde{u})\, \tilde{D}_x (1 - \frac{h^2}{6} D_x^2) T \right\rangle \right| \\
\leq \|T\|_{W^{1,\infty}(\mathcal{M})} \|\tilde{T}\| \|\mathcal{A}_y(\mathcal{A}_z \tilde{u})\| \\
\leq C_1 (\|T_e\|_{C^1} + 1) \|\tilde{T}\| \|\nabla_h \tilde{T}\|_2, \quad \text{(by (5.37) and (5.58))}, \\
\leq \frac{\tilde{C}_2}{\kappa_0} \|\tilde{T}\|^2 + \frac{\kappa_0}{12} \|\nabla_h \tilde{T}\|_2^2, \quad \text{(by Cauchy's inequality)},
\end{aligned}
\tag{5.60}
$$

with $\tilde{C}_2 = C C_1^2 (\|T_e\|_{C^1} + 1)^2$. Similarly, for the second term, we have

$$
\begin{aligned}
\left| \left\langle \tilde{T}, \mathcal{A}_y(\mathcal{A}_z U)\, \tilde{D}_x (1 - \frac{h^2}{6} D_x^2) \tilde{T} \right\rangle \right| \\
\leq \|U\|_{L^\infty} \|\tilde{T}\| \|\nabla_h \tilde{T}\|_2 \\
\leq C (\|T_e\|_{C^1} + 1) \|\tilde{T}\| \|\nabla_h \tilde{T}\|_2, \quad \text{(by (5.23))}, \\
\leq \frac{\tilde{C}_2}{\kappa_0} \|\tilde{T}\|^2 + \frac{\kappa_0}{12} \|\nabla_h \tilde{T}\|_2^2, \quad \text{(by Cauchy's inequality)}.
\end{aligned}
\tag{5.61}
$$

The other terms in Eq. (5.59) can be analyzed in the same manner. Therefore, the combination of Eqs. (5.60) and (5.61) leads to Eq. (5.57). Proposition 5.4 is proven.

$\square$

*Remark 5.5* The reason for the a-priori assumption (5.56) in Proposition 5.4 is to make sure that the $L^\infty$ error of the velocity field is bounded by $Ch$, henceforth bounded by a constant 1. Note that the $L^\infty$ norm of the velocity (both horizontal and vertical)

is bounded by $C/h$ times the $L^\infty$ norm of the temperature, which comes from the recovery formula for the velocity in terms of the temperature gradient. In addition, due to the $O(h^4)$ accuracy in the $L^2$ norm, the $L^\infty$ error of the temperature is bounded by $Ch^{5/2} \leq h^2$, by using an inverse inequality in a 3-D mesh. This avoids the need to perform higher order consistency analysis, which shows another advantage of a fourth-order scheme.

The above argument is valid on some time interval $(0, t_1)$, and the constant $C$ depends on $t_1$. In other words, the convergence analysis provided in this article is for the solution of a fixed final time.

Substituting Eqs. (5.39), (5.47), (5.55) and (5.57) into the energy Eq. (5.38) results in

$$\frac{1}{2}\frac{d}{dt}\|\tilde{T}\|^2 \leq Ch^8 + C\|\boldsymbol{f}_T\|^2 + C\tilde{C}_1\|\tilde{T}\|^2. \tag{5.62}$$

Integrating in time and applying the Gronwall inequality yields

$$\|\tilde{T}\|^2 \leq Ch^8, \tag{5.63}$$

with $C = C(\|T_e\|_{C^{9,\alpha}})$ as introduced in Theorem 3.2 In other words, we have proven that

$$\|T(\cdot, t) - T_e(t)\|_{L^2} \leq Ch^4. \tag{5.64}$$

Using the inverse inequality at the 3-D mesh points gives

$$\|\tilde{T}\|_{L^\infty} \leq C\frac{\|\tilde{T}\|}{h^{3/2}} \leq Ch^{5/2}. \tag{5.65}$$

Consequently, the a-priori assumption (5.56) will never be violated if $h$ is small enough. Theorem 3.2 is proven.                                                                                      $\square$

## References

1. Anderson, C., Reider, M.: A high order explicit method for the computation of flow about a circular cylinder. J. Comput. Phys. **125**, 207–224 (1996)
2. Cao, C.-S., Titi, E.: Global well-posedness and finite-dimensional global attractor for a 3-D planetary geostrophic viscous model. Commun. Pure Appl. Math. **56**, 198–233 (2003)
3. Charney, J.G.: The dynamics of long waves in a baraclinic westerly current. J. Meteorol. **47**, 135–163 (1947)
4. Colin de Verdiere, A.: On mean flow instabilities within the planetary geostrophic equations. J. Phys. Oceanogr. **16**, 1981–1984 (1986)
5. Dukowicz, J., Smith, R., Malone, R.: A reformulation and implementation of the bryan-cox-semtner ocean model on the connection machine. J. Atmos. Ocean. Technol. **10**, 195–208 (1993)

6. E, W., Liu, J.-G.: Essentially compact schemes for unsteady viscous incompressible flows. J. Comput. Phys. **126**, 122–138 (1996)
7. Harlow, F.H., Welch, J.E.: Numerical calculation of time-dependent viscous incompressible flow of fluid with free surface. Phys. Fluids **8**, 2182–2189 (1965)
8. Henshaw, W., Kreiss, H., Reyna, L.: A fourth-order accurate difference approximation for the incompressible Navier–Stokes equations. Comput. Fluids **23**, 575–593 (1994)
9. Lions, J.L., Temam, R., Wang, S.: New formulations of the primitive equations of the atmosphere and applications. Nonlinearity **5**, 237–288 (1992)
10. Liu, J.-G., Samelson, R., Wang, C.: Global weak solution of planetary geostrophic equations with inviscid geostrophic balance. Appl. Anal. **85**, 593–606 (2006)
11. Liu, J.-G., Wang, C., Johnston, H.: A fourth order scheme for incompressible Boussinesq equations. J. Sci. Comput. **18**(2), 253–285 (2003)
12. Liu, J.-G., Wang, W.-C.: An energy-preserving MAC-Yee scheme for the incompressible MHD equation. J. Comput. Phys. **174**, 12–37 (2001)
13. Pedlosky, J.: The equations for geostrophic motion in the ocean. J. Phys. Oceanogr. **14**, 448–455 (1984)
14. Pedlosky, J.: Geophysical Fluid Dynamics, 2nd edn. Springer, New York (1987)
15. Phillips, N.A.: Geostrophic motion. Rev. Geophys. **1**, 123–176 (1963)
16. Robinson, A., Stommel, H.: The oceanic thermocline and associated thermohaline circulation. Tellus **11**, 295–308 (1959)
17. Salmon, R.: The thermocline as an "internal boundary layer". J. Mar. Res. **48**, 437–469 (1990)
18. Samelson, R., Temam, R., Wang, C., Wang, S.: Surface pressure Poisson equation formulation of the primitive equations: Numerical schemes. SIAM J. Numer. Anal. **41**, 1163–1194 (2003)
19. Samelson, R., Temam, R., Wang, S.: Some mathematical properties of the planetary geostrophic equations for large scale ocean circulation. Appl. Anal. **70**, 147–173 (1998)
20. Samelson, R., Temam, R., Wang, S.: Remarks on the planetary geostrophic model of grye scale ocean circulation. Differ. Integral Equ. **13**, 1–14 (2000)
21. Samelson, R., Vallis, G.: A simple friction and diffusion scheme for planetary geostrophic basin models. J. Phys. Oceanogr. **27**, 186–194 (1997)
22. Smith, R., Dukowicz, J., Malone, R.: Parallel ocean general circulation modeling. Phys. D **60**, 38–61 (1992)
23. Stommel, H., Webster, J.: Some properties of the thermocline equations in a subtropical gyre. J. Mar. Res. **44**, 695–711 (1962)
24. Temam, R.: Navier–Stokes Equations: Theory and Numerical Analysis. North-Holland, Amsterdam (1984)
25. Wang, C.: The primitive equations formulated in mean vorticity, Discrete and Continuous Dynamical Systems. In: Proceedings of International Conference on Dynamical Systems and Differential Equations, pp. 880–887 (2003)
26. Wang, C.: Convergence analysis of the numerical method for the primitive equations formulated in mean vorticity on a Cartesian grid. Discret. Contin. Dynam. Syst. Ser. B **4**, 1143–1172 (2004)
27. Wang, C., Liu, J.-G.: Analysis of finite difference schemes for unsteady Navier–Stokes equations in vorticity formulation. Numer. Math. **91**, 543–576 (2002)
28. Wang, C., Liu, J.-G., Johnston, H.: Analysis of a fourth order finite difference method for incompressible Boussinesq equations. Numer. Math. **97**, 555–594 (2004)
29. Welander, P.: An advective model of the ocean thermocline. Tellus **11**, 309–318 (1959)